



# International Agreement Report

## Assessment of TRACE 5.0 against ROSA Test 6-2, Vessel Lower Plenum SBLOCA

Prepared by:  
S. Gallardo, V. Abella, G. Verdú

Universidad Politécnica de Valencia  
ETSII  
Camí de Vera s/n  
46021 Valencia, SPAIN

A. Calvo, NRC Project Manager

**Office of Nuclear Regulatory Research  
U.S. Nuclear Regulatory Commission  
Washington, DC 20555-0001**

**February 2011**

Prepared as part of  
The Agreement on Research Participation and Technical Exchange  
Under the International Code Assessment and Maintenance Program (CAMP)

**Published by  
U.S. Nuclear Regulatory Commission**

**AVAILABILITY OF REFERENCE MATERIALS  
IN NRC PUBLICATIONS**

**NRC Reference Material**

As of November 1999, you may electronically access NUREG-series publications and other NRC records at NRC's Public Electronic Reading Room at <http://www.nrc.gov/reading-rm.html>. Publicly released records include, to name a few, NUREG-series publications; *Federal Register* notices; applicant, licensee, and vendor documents and correspondence; NRC correspondence and internal memoranda; bulletins and information notices; inspection and investigative reports; licensee event reports; and Commission papers and their attachments.

NRC publications in the NUREG series, NRC regulations, and *Title 10, Energy*, in the Code of *Federal Regulations* may also be purchased from one of these two sources.

1. The Superintendent of Documents  
U.S. Government Printing Office  
Mail Stop SSOP  
Washington, DC 20402-0001  
Internet: bookstore.gpo.gov  
Telephone: 202-512-1800  
Fax: 202-512-2250
2. The National Technical Information Service  
Springfield, VA 22161-0002  
[www.ntis.gov](http://www.ntis.gov)  
1-800-553-6847 or, locally, 703-605-6000

A single copy of each NRC draft report for comment is available free, to the extent of supply, upon written request as follows:

Address: Office of the Chief Information Officer,  
Reproduction and Distribution  
Services Section  
U.S. Nuclear Regulatory Commission  
Washington, DC 20555-0001  
E-mail: [DISTRIBUTION@nrc.gov](mailto:DISTRIBUTION@nrc.gov)  
Facsimile: 301-415-2289

Some publications in the NUREG series that are posted at NRC's Web site address <http://www.nrc.gov/reading-rm/doc-collections/nuregs> are updated periodically and may differ from the last printed version. Although references to material found on a Web site bear the date the material was accessed, the material available on the date cited may subsequently be removed from the site.

**Non-NRC Reference Material**

Documents available from public and special technical libraries include all open literature items, such as books, journal articles, and transactions, *Federal Register* notices, Federal and State legislation, and congressional reports. Such documents as theses, dissertations, foreign reports and translations, and non-NRC conference proceedings may be purchased from their sponsoring organization.

Copies of industry codes and standards used in a substantive manner in the NRC regulatory process are maintained at—

The NRC Technical Library  
Two White Flint North  
11545 Rockville Pike  
Rockville, MD 20852-2738

These standards are available in the library for reference use by the public. Codes and standards are usually copyrighted and may be purchased from the originating organization or, if they are American National Standards, from—

American National Standards Institute  
11 West 42<sup>nd</sup> Street  
New York, NY 10036-8002  
[www.ansi.org](http://www.ansi.org)  
212-642-4900

Legally binding regulatory requirements are stated only in laws; NRC regulations; licenses, including technical specifications; or orders, not in NUREG-series publications. The views expressed in contractor-prepared publications in this series are not necessarily those of the NRC.

The NUREG series comprises (1) technical and administrative reports and books prepared by the staff (NUREG-XXXX) or agency contractors (NUREG/CR-XXXX), (2) proceedings of conferences (NUREG/CP-XXXX), (3) reports resulting from international agreements (NUREG/IA-XXXX), (4) brochures (NUREG/BR-XXXX), and (5) compilations of legal decisions and orders of the Commission and Atomic and Safety Licensing Boards and of Directors' decisions under Section 2.206 of NRC's regulations (NUREG-0750).

**DISCLAIMER:** This report was prepared as an account of work sponsored by an agency of the U.S. Government. Neither the U.S. Government nor any agency thereof, nor any employee, makes any warranty, expressed or implied, or assumes any legal liability or responsibility for any third party's use, or the results of such use, of any information, apparatus, product, or process disclosed in this publication, or represents that its use by such third party would not infringe privately owned rights.

---

# Assessment of TRACE 5.0 against ROSA Test 6-2, Vessel Lower Plenum SBLOCA.

## Draft Report for Comment

---

Manuscript Completed: June 2010  
Date Published: February 2011

Prepared by:  
S. Gallardo, V. Abella, G. Verdú

Universidad Politécnica de Valencia  
ETSII  
Camí de Vera s/n  
46021 Valencia, SPAIN

A. Calvo, NRC Project Manager

Prepared for:  
**Division of Systems Analysis**  
**Office of Nuclear Regulatory Research**  
U.S. Nuclear Regulatory Commission  
Washington, DC 20555-0001





## **ABSTRACT**

The purpose of this work is to provide an overview of the results obtained in the simulation of a pressure vessel lower plenum Small Break Loss-Of-Coolant Accident (SBLOCA) under the assumption of total failure of High Pressure Injection System (HPIS) in the Large Scale Test Facility (LSTF) via the thermal-hydraulic code TRACE5.

The work is developed in the frame of OECD/NEA ROSA Project Test 6-2 (SB-PV-10 in JAEA). An asymmetrical steam generator secondary-side depressurization is produced as an accident management action at the steam generator in the loop without PZR, after the generation of the safety injection signal in order to achieve a determined depressurization rate in the primary system. A detailed model has been developed with TRACE5 following these assumptions.

Results of the simulation are compared with the experimental in several graphs, observing an acceptable general behavior in the entire transient. In conclusion, this work represents a small contribution for assessment of the predictability of thermal hydraulic computer codes such as TRACE5.



## FOREWORD

Extensive knowledge and techniques have been produced and made available in the field of thermal-hydraulic responses during reactor transients and accidents, and major system computer codes have achieved a high degree of maturity through extensive qualification, assessment and validation processes. Best-estimate analysis methods are increasingly used in licensing, replacing the traditional conservative approaches. Such methods include an assessment of the uncertainty of their results that must be taken into account when the safety acceptance criteria for the licensing analysis are verified.

Traditional agreements between the Nuclear Regulatory Commission of the United States of America (USNRC) and the Consejo de Seguridad Nuclear of Spain (CSN) in the area of nuclear safety research have given access to CSN to the NRC-developed best estimate thermalhydraulic codes RELAP5, TRAC-P, TRAC-B, and currently TRACE. These complex tools, suitable state-of-the-art application of current two-phase flow fluid mechanics techniques to light water nuclear power plants, allow a realistic representation and simulation of thermalhydraulic phenomena at normal and incidental operation of NPP. Owe to the huge required resources, qualification of these codes have been performed through international cooperation programs. USNRC CAMP program (Code Applications and Maintenance Program) represents the international framework for verification and validation of NRC TH codes, allowing to:

- Share experience on code errors and inadequacies, cooperating in resolution of deficiencies and maintaining a single, internationally recognized code version.
- Share user experience on code scaling, applicability, and uncertainty studies.
- Share a well documented code assessment data base.
- Share experience on full scale power plant safety-related analyses performed with codes (analyses of operating reactors, advanced light water reactors, transients, risk-dominant sequences, and accident management and operator procedures-related studies).
- Maintain and improve user expertise and guidelines for code applications.

Since 1984, when the first LOFT agreement was settled down, CSN has been promoting coordinated joint efforts with Spanish organizations, such as UNESA (the association of Spanish electric energy industry) as well as universities and engineering companies, in the aim of assimilating, applying, improving and helping the international community in the validation of these TH simulation codes<sup>1</sup>, within different periods of the associated national programs (e.g., CAMP-España). As a result of these actions, there is currently in Spain a good collection of productive plant models as well as a good selection of national experts in the application of TH simulation tools, with adequate TH knowledge and suitable experience on their use.

Many experimental facilities have contributed to the today's availability of a large thermal-hydraulic database (both separated and integral effect tests). However there is continued need for additional experimental work and code development and verification, in areas where no emphasis have been made along the past. On the basis of the SESAR/FAP2 reports "Nuclear Safety Research in OECD Countries:Major Facilities and Programmes at Risk" (SESAR/FAP, 2001) and its 2007 updated version "Support Facilities for Existing and Advanced Reactors (SFEAR) NEA/CSNI/R(2007)6", CSNI is promoting since 2001 several collaborative international actions in the area of experimental TH research. These reports presented some findings and recommendations to the CSNI, to sustain an adequate level of research, identifying a number of experimental facilities and programmes of potential interest for present or future international collaboration within the safety community during the coming decade.

CSN, as Spanish representative in CSNI, is involved in some of these research activities, helping in this international support of facilities and in the establishment of a large network of international collaborations. In

---

1 It's worth to note the emphasis made in the application to actual NPP incidents.

2 SESAR/FAP is the Senior Group of Experts on Nuclear Safety Research Facilities and Programmes of NEA Committee on the Safety of Nuclear Installations (CSNI).

the TH framework, most of these actions are either covering not enough investigated safety issues and phenomena (e.g., boron dilution, low power and shutdown conditions), or enlarging code validation and qualification data bases incorporating new information (e.g., multi-dimensional aspects, non-condensable gas effects). In particular, CSN is currently participating in the PKL and ROSA programmes.

The PKL is an important integral test facility operated by of AREVA-NP in Erlangen (Germany), and designed to investigate thermal-hydraulic response of a four-loop Siemens designed PWR. Experiments performed during the PKL/OECD program have been focused on the issues:

- Boron dilution events after small-break loss of coolant accidents.
- Loss of residual heat removal during mid-loop operation (both with closed and open reactor coolant system).

ROSA/LSTF of Japan Atomic Energy Research Institute (JAERI) is an integral test facility designed to simulate a 1100 MWe four-loop Westinghouse-type PWR, by two loops at full-height and 1/48 volumetric scaling to better simulate thermal-hydraulic responses in large-scale components. The ROSA/OECD project has investigated issues in thermal-hydraulics analyses relevant to water reactor safety, focusing on the verification of models and simulation methods for complex phenomena that can occur during reactor transients and accidents such as:

- Temperature stratification and coolant mixing during ECCS coolant injection
- Water hammer-like phenomena
- ATWS
- Natural circulation with super-heated steam
- Primary cooling through SG depressurization
- Pressure vessel upper-head and bottom break LOCA

This overall CSN involvement in different international TH programmes has outlined the scope of the new period of CAMP-España activities focused on:

- Analysis, simulation and investigation of specific safety aspects of PKL/OECD and ROSA/OECD experiments.
- Analysis of applicability and/or extension of the results and knowledge acquired in these projects to the safety, operation or availability of the Spanish nuclear power plants.

Both objectives are carried out by simulating experiments and plant application with the last available versions of NRC TH codes (RELAP5 and TRACE). A CAMP in-kind contribution is aimed as end result of both types of studies.

Development of these activities, technically and financially supported by CSN, is being carried out by 5 different national research groups (Technical Universities of Madrid, Valencia and Cataluña). On the whole, CSN is seeking to assure and to maintain the capability of the national groups with experience in the thermal hydraulics analysis of accidents of the Spanish nuclear power plants.

---

Francisco Fernández Moreno, Commissioner  
Consejo de Seguridad Nuclear (CSN)



# CONTENTS

	<u>Page</u>
<b>Abstract</b> .....	iii
<b>Foreword</b> .....	v
<b>Executive Summary</b> .....	xi
<b>Acknowledgements</b> .....	xiii
<b>Abbreviations</b> .....	xv
<b>1. Introduction</b> .....	1-1
<b>2. ROSA LSTF description</b> .....	2-1
<b>3. Transient description</b> .....	3-1
<b>4. Applied method: TRACE5 model of ROSA LSTF</b> .....	4-1
<b>5. Results and discussion</b> .....	5-1
5.1. Steady-state .....	5-1
5.2. Transient .....	5-2
5.3. System pressures .....	5-4
5.4. Break.....	5-6
5.5. Primary loops mass flow .....	5-7
5.6. Vessel collapsed liquid levels .....	5-10
5.7. Peak cladding temperature .....	5-13
5.8. Hot and cold legs liquid levels.....	5-14
5.9. Steam generator main steam mass flow rate.....	5-18
5.10. Steam generator relief valve flow rate.....	5-20
5.11. Steam generator u-tubes collapsed liquid level .....	5-22
5.12. Steam generators secondary-side liquid level .....	5-26
5.13. Pressurizer liquid level .....	5-28
5.14. Accumulator liquid level .....	5-29
5.15. Hot leg temperature .....	5-30
5.16. Downcomer fluid temperature .....	5-31
<b>6. Conclusions</b> .....	6-1
<b>8. References</b> .....	7-1

## Figures

	<u>Page</u>
Figure 1 Model nodalization used for simulation.....	4-1
Figure 2 3D Vessel nodalization and connections visualized with SNAP .....	4-2
Figure 3 Steam generator nodalization.....	4-3
Figure 4 Primary and secondary pressures (0.0 to 1.0 NT).....	5-5
Figure 5 Primary and secondary pressures (0.0 to 0.25 NT).....	5-5
Figure 6 Break mass flow rate (0.0 to 1.0 NT).....	5-6
Figure 7 Discharged inventory through the break (0.0 to 1.0 NT).....	5-7
Figure 8 Primary mass flow, loop A (0.0 to 1.0 NT) .....	5-8
Figure 9 Primary mass flow, loop A (0.0 to 0.2 NT) .....	5-8
Figure 10 Primary mass flow, loop B (0.0 to 1.0 NT) .....	5-9
Figure 11 Primary mass flow, loop B (0.0 to 0.4 NT) .....	5-9
Figure 12 Upper plenum collapsed liquid level (0.0 to 1.0 NT).....	5-10
Figure 13 Upper plenum collapsed liquid level (0.0 to 0.5 NT).....	5-11
Figure 14 Core collapsed liquid level (0.0 to 1.0 NT).....	5-11
Figure 15 Downcomer collapsed liquid level (0.0 to 1.0 NT) .....	5-12
Figure 16 Upper head collapsed liquid level .....	5-12
Figure 17 Maximum fuel rod surface temperature .....	5-13
Figure 18 Core power (0.0 to 1.0 NT) .....	5-14
Figure 19 Collapsed liquid level in hot leg A (0.0 to 1.0 NT).....	5-15
Figure 20 Collapsed liquid level in hot leg A (0.0 to 0.4 NT).....	5-15
Figure 21 Collapsed liquid level in hot leg B (0.0 to 1.0 NT).....	5-16
Figure 22 Collapsed liquid level in hot leg B (0.0 to 0.4 NT).....	5-16
Figure 23 Collapsed liquid level in cold leg A (0.0 to 1.0 NT) .....	5-17
Figure 24 Collapsed liquid level in the cold leg B (0.0 to 1.0 NT) .....	5-17
Figure 25 Steam mass flow through the main line (0.0 to 1.0 NT).....	5-18
Figure 26 Steam mass flow through the main line (0.0 to 0.1 NT).....	5-18
Figure 27 Steam mass flow through the main line (0.0 to 1.0 NT).....	5-19
Figure 28 Steam mass flow through the main line (0.0 to 0.1 NT).....	5-19
Figure 29 SG A relief valve mass flow rate (0.0 to 1.0 NT).....	5-20
Figure 30 SG A relief valve mass flow rate (0.0 to 0.2 NT).....	5-21
Figure 31 SG B relief valve mass flow rate (0.0 to 1.0 NT).....	5-21

Figure 32	SG B relief valve mass flow rate (0.0 to 0.2 NT).....	5-22
Figure 33	Collapsed liquid level in the U-tubes of the SG A. Inlet (0.0 to 1.0 NT).....	5-23
Figure 34	Collapsed liquid level in the U-tubes of the SG A. Inlet (0.0 to 0.3 NT).....	5-23
Figure 35	Collapsed liquid level in the U-tubes of the SG A. Outlet (0.0 to 1.0 NT) .....	5-24
Figure 36	Collapsed liquid level in the U-tubes of the SG A. Outlet (0.0 to 0.3 NT) .....	5-24
Figure 37	Collapsed liquid level in the U-tubes of the SG B. Inlet (0.0 to 1.0 NT).....	5-25
Figure 38	Collapsed liquid level in the U-tubes of the SG B. Outlet (0.0 to 1.0 NT) .....	5-25
Figure 39	Steam generator A. Secondary-side collapsed liquid level (0.0 to 1.0 NT) .....	5-26
Figure 40	Steam generator A. Secondary-side collapsed liquid level (0.0 to 0.2 NT) .....	5-27
Figure 41	Steam generator B. Secondary-side collapsed liquid level (0.0 to 1.0 NT) .....	5-27
Figure 42	Steam generator B. Secondary-side collapsed liquid level (0.0 to 0.4 NT) .....	5-28
Figure 43	PZR liquid level.....	5-29
Figure 44	Accumulator liquid level in loop A .....	5-29
Figure 45	Accumulator liquid level in loop B .....	5-30
Figure 46	Maximum hot leg fluid temperature .....	5-30
Figure 47	Downcomer fluid temperature (level 5.5 m).....	5-31

## Tables

	<u>Page</u>
Table 1. Control logic and sequence of major events in the experiment .....	3-1
Table 2. Predetermined core power decay curve .....	3-2
Table 3. Pumps relative rotational speed .....	3-3
Table 4. Curve of predetermined pressure drop after the beginning of the AM management action in the secondary-side of the steam generator in the loop without PZR.....	3-3
Table 5. Core protection system logic.....	3-4
Table 6. Number of heaters per heat structure .....	4-3
Table 7. Steady-state condition. Comparison between experimental and simulated values.....	5-1
Table 8. Chronological sequence of events. Comparison between experiment and TRACE .....	5-3

## **EXECUTIVE SUMMARY**

The purpose of this work is to provide an overview of the results obtained in the simulation of a pressure vessel lower plenum Small Break Loss-Of-Coolant Accident (SBLOCA) under the assumption of total failure of High Pressure Injection System (HPIS) in the Large Scale Test Facility (LSTF) via the thermal-hydraulic code TRACE5.

The work is developed in the frame of OECD/NEA ROSA Project Test 6-2 (SB-PV-10 in JAEA). An asymmetrical steam generator secondary-side depressurization is produced as an accident management action at the steam generator in the loop without PZR, after the generation of the safety injection signal in order to achieve a determined depressurization rate in the primary system. A detailed model has been developed with TRACE5 following these assumptions.

Results of the simulation are compared with the experimental in several graphs, observing an acceptable general behaviour in the entire transient. In conclusion, this work represents a small contribution for assessment of the predictability of thermal hydraulic computer codes such as TRACE5.



## **ACKNOWLEDGEMENTS**

This paper contains findings that were produced within the OECD-NEA ROSA Project. The authors are grateful to the Management Board of the ROSA Project for their consent to this publication, and thank the Spanish Nuclear Regulatory Body (CSN) for the technical and financial support under the agreement STN/1388/05/748.





## ABBREVIATIONS

ACC	Accumulator
AFW	Auxiliary Feed Water
AIS	Accumulator Injection System
AM	Accident Management
CCFL	Counter-current Flow Limiting
CP	Coolant Pump
ECCS	Emergency Core Cooling System
HPI	High Pressure Injection
JAEA	Japan Atomic Energy Agency
JC	Jet Condenser
LSTF	Large Scale Test Facility
LPI	Low Pressure Injection System
MFW	Main Feed Water
MSIV	Main Steam Isolation Valve
PCT	Peak Cladding Temperature
PGIT	Primary Gravity Injection Tank
PV	Pressure Vessel
PWR	Pressurized Water Reactor
PZR	Pressurizer
RHR	Residual Heat Removal
RV	Relief Valve
SBLOCA	Small Break Loss-of-coolant Accident
SG	Steam Generator
ST	Storage Tank



# 1 INTRODUCTION

When a Loss-Of-Coolant Accident (LOCA) in a PWR reactor occurs, the Emergency Core Cooling System (ECCS) automatically actuates. ECCS, for a Westinghouse-type PWR, consists of three injection systems: High Pressure Injection (HPI) system, accumulator (ACC) injection system, and Low Pressure Injection (LPI) system. These systems are activated successively as the primary pressure decreases. However, the reactor coolant inventory can keep on decreasing if HPI system fails during a Small Break LOCA (SBLOCA) with a break discharge flow rate too small to depressurize the primary system to the ACC injection pressure. In this frame, an intentional asymmetrical depressurization of one Steam Generator (SG) secondary-side, by means of an Accident Management (AM) action is studied. The main goal of the experiment is to determine if this depressurization is able to achieve a primary system cooling rate of -55 K/h and therefore, if this action is enough to ensure the core cooling in case of nitrogen gas inflow in the primary circuit. The advantage of this procedure over the primary-side steam relief is that it does not cause loss of the reactor coolant inventory.

In addition, in the last years, there has been a significant interest in the development of codes and methodologies for “best-estimate” analysis of LOCAs, as it can be found in the literature [7, 9-15]. Extensive research activities have been performed to develop thermalhydraulic codes, such as RELAP5 [6], ATHLET [7] and CATHARE [8], which enable a more realistic simulation of nuclear reactor systems.

The aim of the present work is to describe the main results achieved by the authors using the thermal-hydraulic code TRACE5 [4, 5], in the frame of OECD/NEA ROSA Project Test 6-2 (SB-PV-10 in JAEA) [1], with the purpose of testing the behaviour of the code for this transient. A post-test analysis was performed with the main objective of assessing the code's capability in predicting the thermal-hydraulic responses to the simulated secondary-side depressurization procedure. The experiment 6-2 of the OECD/NEA ROSA project was conducted during 15th and 16th of December, 2005 in the Large Scale Test Facility (LSTF) [3] of the Japanese Atomic Energy Agency (JAEA) [1, 2]. The LSTF simulates a PWR reactor, Westinghouse type, of four loops and 3423 MW of thermal power, scaled to 1/48 in volume and two loops. The experiment simulates a SBLOCA in the lower plenum of the pressurized vessel.



## 2 ROSA LSTF DESCRIPTION

This section consists in a sketched description of the LSTF facility (in the Tokai Research Establishment of the JAEA) [3]. Two loops compose the primary coolant system: the primary loop A with the pressurizer (PZR) and the symmetrical primary loop B. Both include a primary coolant pump (PC) and a steam generator (SG). On the other hand, the secondary-coolant system includes a jet condenser (JC), a feedwater pump (PF), the auxiliary feedwater pumps (PA) and two SG secondary systems with a related piping system.

The ECCSs consist of the following sub-systems: the high pressure charging pump (PJ), the high pressure injection pump (PL), the residual heat removal (RHR) system and the primary gravity injection tank (PGIT). A break flow storage tank (ST) stores the discharged coolant from the primary system.

The pressure vessel (PV) is composed of the following elements: The upper head located above the upper core support plate; the upper plenum situated between the upper core support plate and the upper core plate; the core; the lower plenum and the downcomer annulus region which surrounds the core and upper plenum. LSTF vessel is structured with 8 spray nozzles (of 3.4 mm inner-diameter) at the upper head, and 8 control rod guide tubes (CRGTs) which lead the flow path between the upper head and the upper plenum.

Each steam generator (SG) contains 141 U-tubes grouped depending on their length (an average length of 19.7 m can be considered, with a maximum height of 10.62 m and a minimum height of 9.156 m). All the U-tubes are characterized with an inner diameter of 19.6 mm and an outer diameter of 25.4 mm (2.9 mm of wall thickness). The total inner and outer surface areas are therefore 171 and 222 m<sup>2</sup>, respectively. Regarding to the vessel, plenum and riser of steam generators, the inner heights are 19.840, 1.183 and 17.827 m, respectively. The downcomer is 14.101 m.



### 3 TRANSIENT DESCRIPTION

The control logic of the transient is listed in Table 2. The break unit is connected to the PV lower plenum nozzle at 1.735 m below the core bottom elevation. After the break started, the primary coolant was discharged through the break and accumulated in the storage tank.

The experiment was initiated by quickly opening the break valve at time zero. The inner diameter of the break is 3.2 mm, satisfying the assumption of 0.1% of the size of the cold leg. Simultaneously, rotational speed of primary coolant pumps was increased up to 1500 rpm. A scram signal was generated when the PZR pressure dropped below a determined value. This signal produces the initiation of the core power decay curve, calculated by considering the stored heat in fuel rods and delayed neutron fission power, as it can be seen in Table 2. The initial core power corresponds to 14% of the nominal power of a PWR volumetrically scaled (1/48). When liquid level PZR is lower than certain height, heaters (backup and proportional) are turned off. NT stands for Normalized Time and NV for Normalized Value.

**Table 1 Control logic and sequence of major events in the experiment**

Event	Condition
Break.	Time zero.
Generation of scram signal.	Primary pressure drops to 0.81 NV.
PZR heaters off.	Generation of scram signal or PZR liquid level below 0.306 NV.
Initiation of the core power decay curve.	Generation of scram signal.
Initiation of primary pumps stopping curve.	Generation of scram signal.
Turbine signal (turbine trip).	Generation of scram signal.
Main steam isolation valve (MSIV) closure.	Generation of scram signal.
Feed water termination.	Generation of scram signal.
Generation of safety injection (SI) signal.	Primary pressure drops to 0.76 NV.
Initiation of auxiliary feed water.	Generation of safety injection SI signal.
Asymmetrical depressurization at the secondary of the steam generator in the loop without PZR.	Little after the generation of the SI signal.
Initiation of the accumulation system.	Primary pressure drops to 0.28 NV.
Initiation of low pressure injection system.	Pressure of the lower plenum of the vessel below 0.07 NV.

**Table 2 Predetermined core power decay curve**

Normalized Time	Normalized Power	Normalized Time	Normalized Power
0	1	0.0033	0.3042
0.00075	1	0.0042	0.2763
0.00083	0.8150	0.0063	0.2423
0.0013	0.5366	0.0083	0.2263
0.0017	0.4504	0.0125	0.2079
0.0021	0.3906	0.0167	0.2000
0.0025	0.3538	0.0208	0.1913

Normalized Time	Normalized Power	Normalized Time	Normalized Power
0.025	0.1832	0.208	0.0936
0.033	0.1577	0.25	0.0886
0.0417	0.1487	0.33	0.0814
0.0625	0.1342	0.41	0.0763
0.0833	0.1238	0.83	0.0629
0.125	0.1096	-	-
0.166	0.1003	-	-

At the same time, the primary coolant pump coastdown is initiated, also using a pre-determined rotational speed curve (Table 3). Pumps are completely stopped 0.01NT after scram signal generation.



**Table 3 Pumps relative rotational speed**

Normalized Time	Relative rotational	Normalized Time	Relative rotational	Normalized Time	Relative rotational
0	1.000	0.0013	0.280	0.0033	0.125
0.000083	0.850	0.0017	0.220	0.0037	0.110
0.000208	0.730	0.0021	0.185	0.0042	0.100
0.00041	0.540	0.0025	0.160	0.0104	0.000
0.00083	0.370	0.0029	0.140	--	---

A turbine trip is activated by closing the steam generators Main Steam Isolation Valves (MSIVs). The closure of MSIVs produces an increasing of SG secondary-side pressure and a temporary rise in primary pressure, followed by a new decrease due to core power decay effect. Simultaneously, main feedwater flow of both steam generators is stopped. The Safety Injection (SI) signal is generated when the primary pressure decreased to a determined value. From this moment on, the Relief Valves (RV) in both SGs, begin opening and closing in order to maintain the pressure between two fixed values.

Around 0.0012 NT after the SI signal, the action of asymmetrical depressurization in the secondary-side of the SG B (in loop without PZR) begins in order to achieve a depressurization rate of -55 K/h in the primary system. This depressurization is produced by closing the RV and gradually opening the manually operated valve (MV), according to a pre-determined pressure drop curve (see Table 4). On the contrary, the relief valve of Steam Generator A (loop with PZR) is closed after initiation of the accident management action.

**Table 4 Curve of predetermined pressure drop after the beginning of the AM management action in the secondary-side of the steam generator in the loop without PZR**

Normalized time	Normalized Value (pressure)	Normalized time	Normalized Value (pressure)	Normalized time	Normalized Value (pressure)
0	0.504	0.0013	0.329	0.0031	0.161
0.000041	0.496	0.0019	0.261	0.0037	0.122
0.00062	0.409	0.0025	0.209	0.0044	0.094

When primary pressure drops to 0.28 NV, the accumulator system starts to inject water in cold legs. In the last part of the experiment, nitrogen gas is injected in both cold legs, throughout the accumulators. Finally, when primary pressure drops to 0.07 NV, the Low Pressure Injection System (LPIS) is initiated.

In order to protect the facility, the core power is automatically decreased by the core protection system when the maximum fuel rod surface temperature excess 958 K, as it can be seen in Table 5.

**Table 5 Core protection system logic**

Control of core power to	Maximum fuel rod surface temperature (K)
75%	958
50%	968
25%	969
10%	970
0%	973

## 4 APPLIED METHOD: TRACE5 MODEL OF ROSA LSTF

TRACE5 code is designed to perform best-estimate analyses of LOCAs or operational transients. However, it has some limitations in use; for example, those transients in which one expects to observe thermal stratification of the liquid phase in the 1D components cannot be directly modeled. Furthermore, it is not appropriate for modeling situations in which transfer of momentum plays an important role at a localized level [4]. In this work, the LSTF has been modeled with 88 hydraulic components (7 BREAKs, 13 FILLs, 29 PIPES, 2 PUMPS, 1 PRIZER, 21 TEEs, 14 VALVES and 1 VESSEL). In order to characterize the heat transfer processes, 48 Heat Structure components (Steam Generator U-tubes, core power, PZR heaters and heat losses) have been considered. Figure 1 shows the nodalization of the model using SNAP (Symbolic Nuclear Analysis Package software).

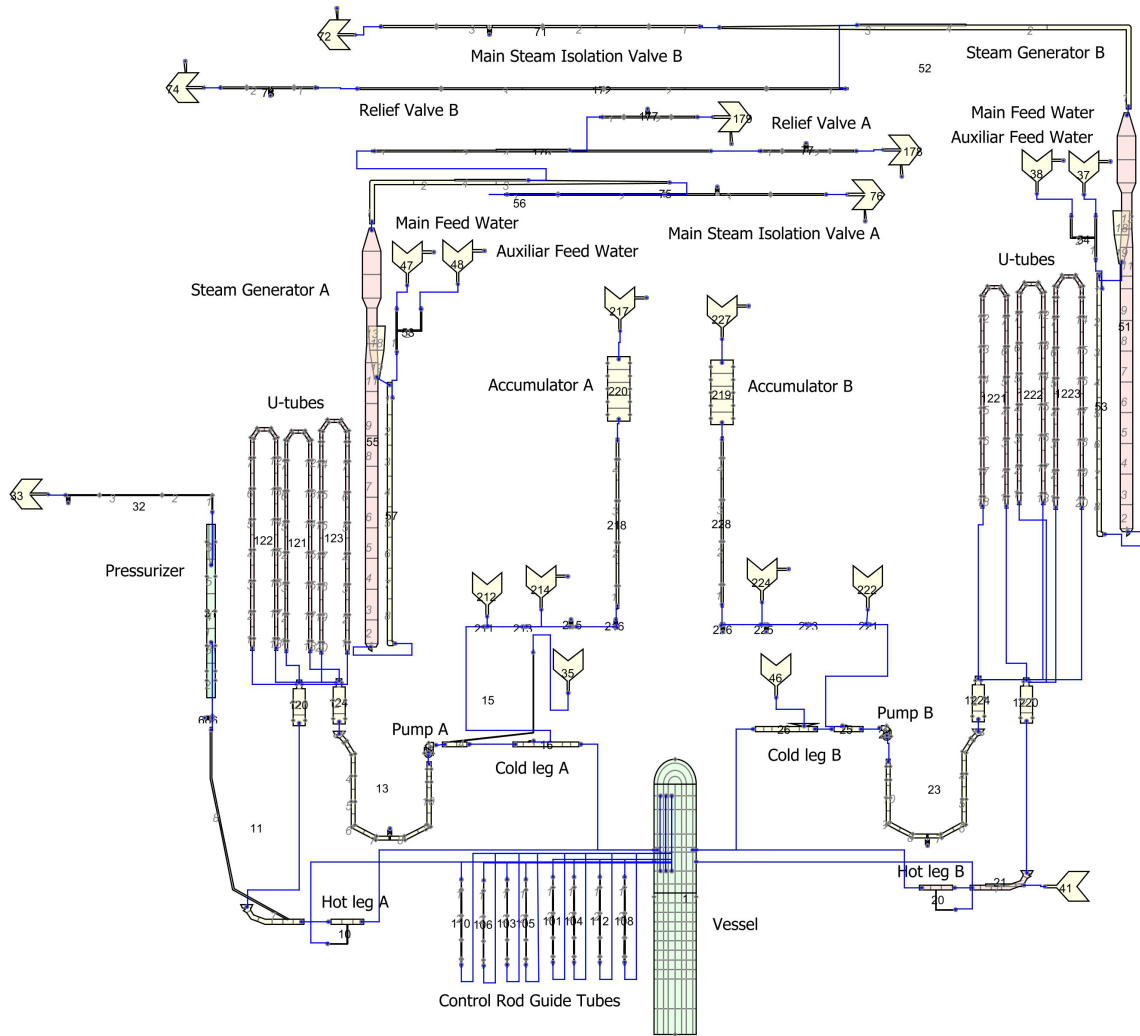
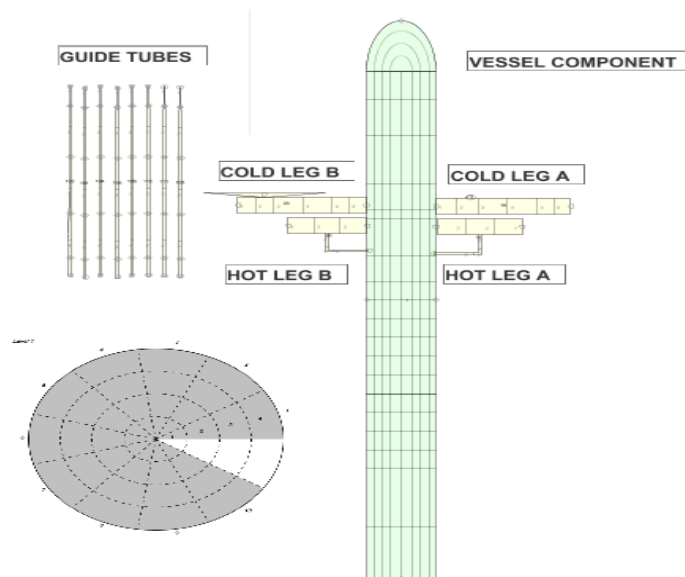


Figure 1 Model nodalization used for simulation

In order to model the pressure vessel, a 3D-VESSEL component has been considered (Figure 2). A nodalization consisting of 19 axial levels, 4 radial rings and 10 azimuthal sectors has been selected. This nodalization characterizes with an acceptable detail the actual features of the LSTF vessel. Increasing the number of axial levels, azimuthal sectors or radial rings, does not improve significantly the agreement with experimental results, but increases CPU time. For each axial level, volume and effective flow area fractions have been set according to technical specifications provided by the organization [3]. Active core is located between levels 3 and 11. Level 12 simulates the upper core plate. Levels 13 to 15 characterize the vessel upper plenum. The upper core support plate is located in level 16. Finally, upper head is defined between levels 17 to 19. 3D-VESSEL is connected to different 1D components: 8 Control Rod Guide Tubes (CRGT), hot leg A and B (level 15), cold leg A and B (level 15) and a bypass channel (level 14). Control rod guide tubes have been simulated by PIPEs components, connecting levels 13 and 19 and allowing the flow between upper head and upper plenum.



**Figure 2 3D Vessel nodalization and connections visualized with SNAP**

30 HTSTRs simulate the fuel assemblies in the active core. A POWER component controls the power supplied by each HTSTR to the 3D-VESSEL. Fuel elements (1008 in total) were distributed into the 3 rings: 154 elements in ring 1, 356 in ring 2 and 498 in ring 3 and also characterized by HTSTR components. In both axial and radial direction, peaking factors were considered. The power ratio in the axial direction presents a peaking factor of 1.495. On the other hand, depending on the radial ring, different peaking factors were considered (0.66 in ring 1, 1.51 in ring 2 and 1.0 in ring 3). The number of fuel rod components associated with each heat structure has been determined from the technical documentation given, taking into account the distribution of fuel rod elements in the vessel, as it can be seen in Table 6.

**Table 6 Number of heaters per heat structure**

HTSTR	Number of heaters	HTSTR	Number of heaters	HTSTR	Number of heaters
310	17	320	44	330	60
311	17	321	40	331	54
312	10	322	23	332	32
313	12	323	32	333	45
314	20	324	40	334	56
315	17	325	42	335	61
316	16	326	38	336	57
317	12	327	26	337	31
318	14	328	30	338	45
319	17	329	39	339	57

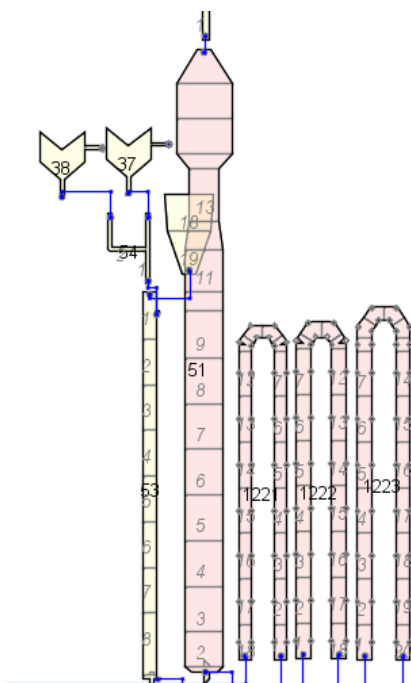


**Figure 3 Steam generator nodalization**

A detailed model of SG (geometry and thermal features) has been developed, due to the fact that TRACE5 does not include any pre-determined steam generator component. A representation of the SG nodalization can be seen in Figure 3. Both boiler and downcomer components of secondary-side have been modelled by TEEs components. U-tubes have been classified into three groups according to each average length and heat transfer features. Steam-separator model can be invoked in TRACE5 setting a friction coefficient (FRIC) greater than 1022 at a determined cell edge, allowing only gas phase to flow through the cell interface. Heat transfer between primary and secondary sides has been performed by using HTSTR components. Cylindrical-shape geometry has been used to best fit heat transmission. Critical heat flux flag has been set in order to use an AECL-IPPE table, calculating critical quality from Biasi correlation [4, 5]. Inner and outer surface boundary conditions for each axial level has been set to couple HTSTR component to hydro components (primary and secondary fluids). Different models varying the number of U-tube groups were tested (1, 3 and 6 groups). It was found that results do not apparently change, using these models. However, in order to best fit the collapsed liquid level in U-tubes without drastically increasing CPU time, a 3-group configuration was finally chosen. Heat losses to environment have been added to secondary-side walls.

Regarding to the break simulation, it is important to take into account the necessity of activating the Choke flow model in the break when critical flow conditions are expected to appear. Choke model predicts for a given cell the conditions for which choked flow is expected to occur, providing three different models in one: subcooled-liquid, two-phase and single-phase vapor model. The break has been simulated by means of a VALVE component connected to a BREAK component in order to establish the boundary conditions. This BREAK has been modelled following the recommendations of the TRACE5 user's manual [5]. In this case, since the break is simulated to discharge in a big volume space (the storage tank), a  $dxin=1.0 \cdot 10^{-6}$  (length) and a  $volin=1.0 \cdot 10^6$  (volume) has been selected with the purpose of providing a large area.

## 5 RESULTS AND DISCUSSION

### 5.1 Steady-state

Steady-state conditions achieved in the simulation were in reasonable agreement with the experimental values. In Table 7, the relative errors (%) between experimental and simulated results for different items are listed. It is important to remark that in any case, the maximum difference between experiment and simulation is 5%. In order to achieve the steady state conditions, the duration of simulation was stated to 5000 seconds.

**Table 7 Steady-state condition. Comparison between experimental and simulated values**

Item	Relative Error (%) (Loop with PZR)
Core Power	0.0
Hot leg Fluid Temperature	0.1
Cold leg Fluid Temperature	0.1
Mass Flow Rate	5.0
PZR Pressure	0.2
PZR Liquid Level	4.3
Accumulator System Pressure	0.2
Accumulator System Temperature	0.5
SG Secondary-side Pressure	0.7
SG Secondary-side Liquid Level	3.8
Steam Flow Rate	0.4
Main feedwater Flow Rate	0.0
Main feedwater Temperature	0.3
Auxiliary Feedwater Temperature	0.3

## 5.2 Transient

In order to analyze results, the full transient has been divided into three phases, each of them characterized by a significant action or event. The first one, from 0 to 0.101 NT, starts at time 0 when the break is produced and finishes when the Accident Management (AM) action is initiated. The following phase consists of a long depressurization process promoted by an asymmetrical steam generator depressurization action (0.101 -0.401NT). In the third part of the transient, the depressurization process is degraded by the non-condensable gas inflow from the Accumulator Injection System AIS tanks before the LPI actuation (0.401-0.961 NT). LPI produces a repeated core quench process.

Table 8 lists the chronology sequence of events during the transient and the comparison in Normalized Time (1 NT = Total Transient Time) between the experiment and TRACE results.

Variables presented in this section follow the requirements for an exhaustive analysis of the transient. The most important parameters that will be studied in this paper are the following: Pressures at both primary and secondary circuits, mass flow rate and discharge coolant inventory through the break, primary mass flow, vessel collapsed-liquid levels, maximum fuel rod surface temperature, core exit temperature, collapsed-liquid levels in hot and cold legs, mass flow in SG relief valves, liquid level in SG secondary-side and liquid level in the accumulators.



**Table 8 Chronological sequence of events. Comparison between experiment and TRACE**

Event	Experiment. Normalized Time (s)	TRACE. Normalized Time (s)
Break.	0	0
Power increase of the proportional heaters of the PZR.	0.00008	0.00008
Power increase of the base heaters of the PZR.	0.0006	0.00064
PZR heaters turned off due to low water level.	0.0134	0.014
Scram signal generation (primary pressure drops to a determined value).	0.0227	0.0222
Pumps predetermined stopping curve initiation.	0.0228	0.023
Core power decay curve initiation.	0.0235	0.023
SI signal generation (primary pressure drops to a determined value).	0.0294	0.0292
Pumps stop.	0.0328	0.0328
Steam generator in loop without PZR depressurization	0.101	0.101
Closure of Relief Valve at both loops with and without PZR.	0.107	0.106
End of Auxiliary feed water in SG in loop with PZR.	0.105	0.105
Change of phase in break mass flow (from liquid to two- phase)	0.178	0.196
Initiation of accumulator injection to cold leg in loop with PZR.	0.204	0.204
Initiation of accumulator injection to cold leg in loop without PZR.	0.205	0.204
Initiation of nitrogen gas injection to the cold leg of loop with PZR.	0.401	0.382
Initiation of nitrogen gas injection to the cold leg of loop without PZR.	0.442	0.383
Initiation of Low Pressure Injection.	0.900	Not reached

### 5.3 System pressures

Figure 4 compares the primary and secondary pressures. The primary pressure begins to decrease at time zero (when the break is produced). In the experiment, the scram signal is generated at 0.0234 NT after the break, when the primary pressure decreases to 0.81 NV (Normalized Value). The generation of the scram signal causes the MSIV of steam generators to close and the beginning of the primary coolant pumps coastdown. The SI signal is generated at 0.0294 NT when the primary pressure decreases to a determined value. The secondary pressure increases rapidly during a short time after the closure of the MSIVs. From this moment on, the secondary pressure starts to oscillate between 0.501 NV and 0.488 NV by means of opening and closing the relief valves (RV) of steam generators, allowing a mass flow rate of 0.48 NV to flow through RVs.

In the second part of the transient, a controlled depressurization of the secondary side of SG B (in loop without PZR) is produced. At same time, relief valve of SG A is fully closed. Behavior of SG A and SG B are completely different, due to the accident management action itself. SG B secondary pressure began to decrease after the AM action started. On the other hand, the SG A secondary pressure temporarily increased after the closure of SG RV because of a continued primary-to-secondary heat transfer while the secondary pressure is lower than the primary pressure. After a delay, primary pressure begins following the pressure drop of the SG B secondary-side due to single-phase liquid natural circulation. Approximately, at 0.16 NT, starts a two-phase natural circulation flow, decreasing primary pressure. At this time, SG A secondary pressure gradually decreased and remained high the rest of the transient. The slight loss of pressure in SGA is due to thermal contraction of coolant and heat losses to environment. Furthermore, depressurization of SG B strongly depends on the predetermined pressure drop curve established by the accident management action.

The good agreement between both experimental and simulated secondary pressures has been achieved by introducing the appropriate opening sequence of the accident management valve (AM valve).

Accumulator system is initiated at about 0.204 NT when the primary pressure decreased to 0.28 NV. The coolant injection from the accumulator system was finished when the primary pressure decreased to 0.1 NV, followed by the discharge of nitrogen gas from the accumulator tanks. TRACE reproduces adequately the liquid level decrease of accumulators (as will be presented in other section) and the entrance of nitrogen gas. Approximately, at 0.44 NT accumulators get completely empty and nitrogen-gas starts to get injected into both cold legs. In the experiment, an accumulation of non-condensable gas is produced in the top of the U-tubes, causing two consecutive temporal increasing in pressure. On the contrary, the SGB secondary pressure slightly decreased when the primary pressure increased. This effect has not been reproduced by TRACE5 because nitrogen transport is characterized with the same equations than water vapor-phase.

When vessel lower plenum pressure reached a determined value, the low pressure injection (LPI) system actuated at about 0.96 NT (in the experiment) but this low pressure value was not reached in the simulation, given as a result the no actuation of the LPI system. This lack of inventory in the system can be seen in Figures 14 and 15 (PV core and upper plenum collapsed liquid level, respectively).

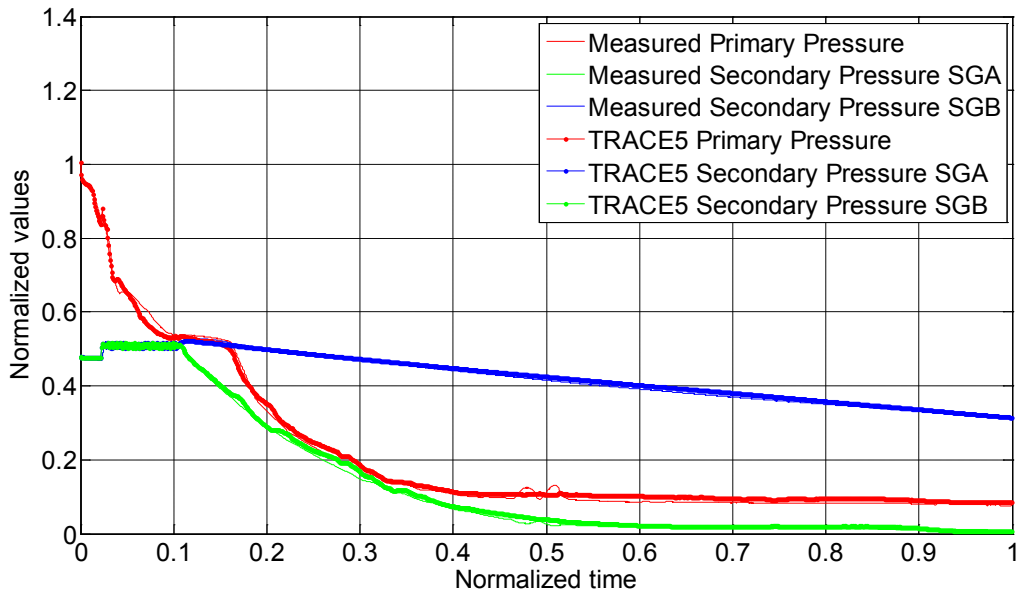


**Figure 4 Primary and secondary pressures (0.0 to 1.0 NT)**

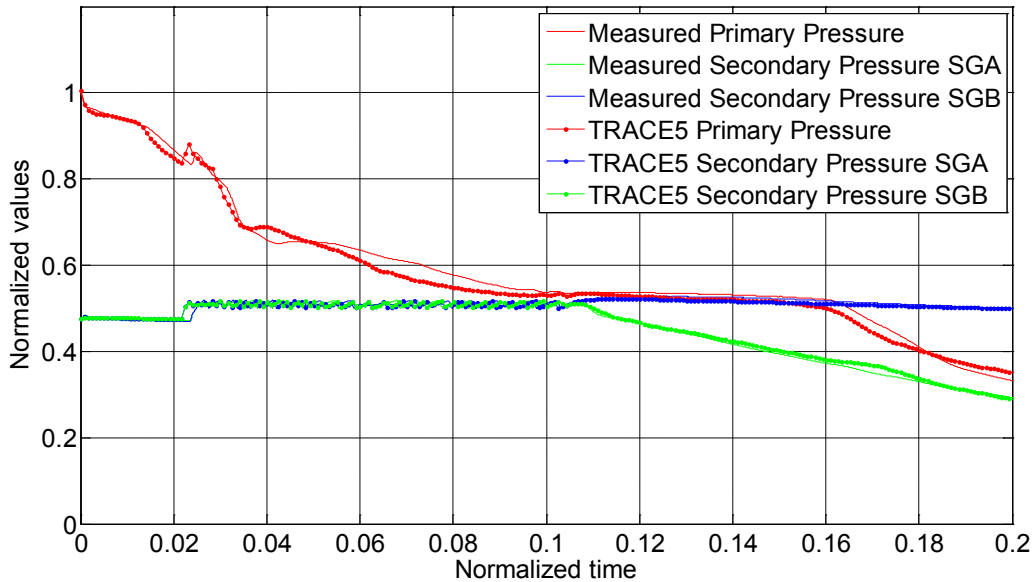


**Figure 5 Primary and secondary pressures (0.0 to 0.25 NT)**

In general, TRACE5 reproduces successfully the pressure evolution during the whole transient. The main disagreements are found during the nitrogen flowing in the primary circuit, especially in the circulation through the U-tubes.

## 5.4 Break

Figures 6 and 7 show the mass flow through the break and the coolant inventory, respectively. Experimentally, mass flow in the break is obtained from the liquid level in the break flow storage tank. In order to adjust the break mass flow and the discharged primary coolant inventory with TRACE, a sensitivity analysis varying the discharge coefficient was performed. A discharge coefficient of 0.78, using Choked flow model [4, 5], fits successfully both mass flow break and discharged coolant inventory. TRACE5 estimates a change of flow from liquid single-phase to two-phase at around 0.16 NT, which completely agrees with the experimental measurements. A proper adjust of the discharged mass flow inventory gives a high reliability to the TRACE model. At this point is very important to remark the conditions at which the discharge is carried out with TRACE. The break has been simulated throughout a PIPE component, which connects with a VALVE component and finally a BREAK in order to establish the boundary conditions. The BREAK has been modelled following the recommendations of the user's guide of TRACE.

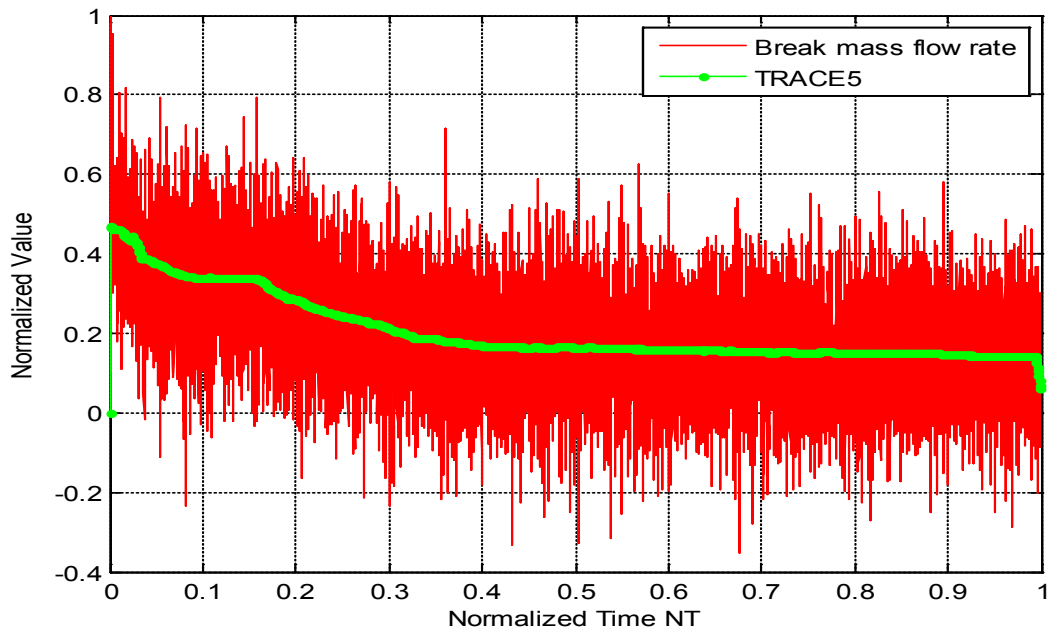


**Figure 6 Break mass flow rate (0.0 to 1.0 NT)**

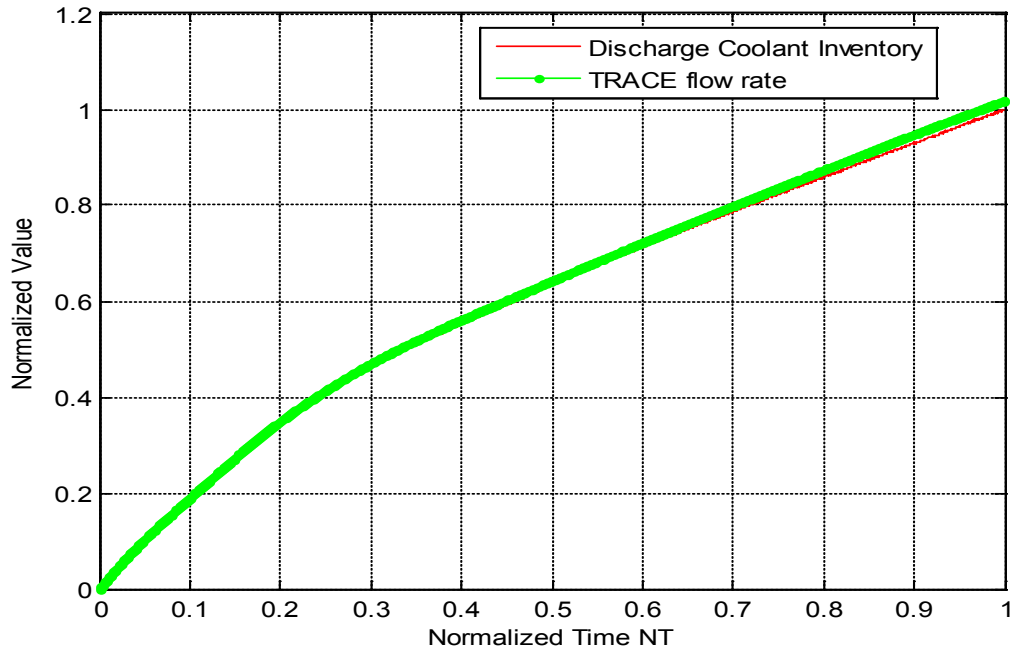


**Figure 7 Discharged inventory through the break (0.0 to 1.0 NT)**

## **5.5 Primary loops mass flow**

Primary mass flow in loop A and B are shown in figures 8, 9, 10 and 11. The initial steady state flows were rapidly increased by primary coolant pumps (PC) at the break time and were maintained at 1 NV in each loop until the start of pump coast-down. In the first part of the transient, mass flow starts to decrease due to the pump coast-down. After the pumps were stopped, only natural circulation flow in each loop contributed to cool down the core. The primary coolant mass gradually decreased according to the break flow. Loop A and B begin to register different flow conditions after the AM action, flow stagnation in loop A and natural circulation flow in loop B, producing an asymmetric coolant mass flow rate in the primary loops. Different loop flow conditions are well predicted by TRACE5.

At 0.2 NT approximately, accumulators start to inject cold water in primary loops. When accumulators become completely empty, starts a continuous nitrogen injection in the system. Coincident with the nitrogen entrance, some fluctuations appear in the mass flow in loop B calculated by TRACE5. Furthermore, calculation time becomes lower when nitrogen is injected in the system. In general, all tendencies are well reproduced by TRACE5.

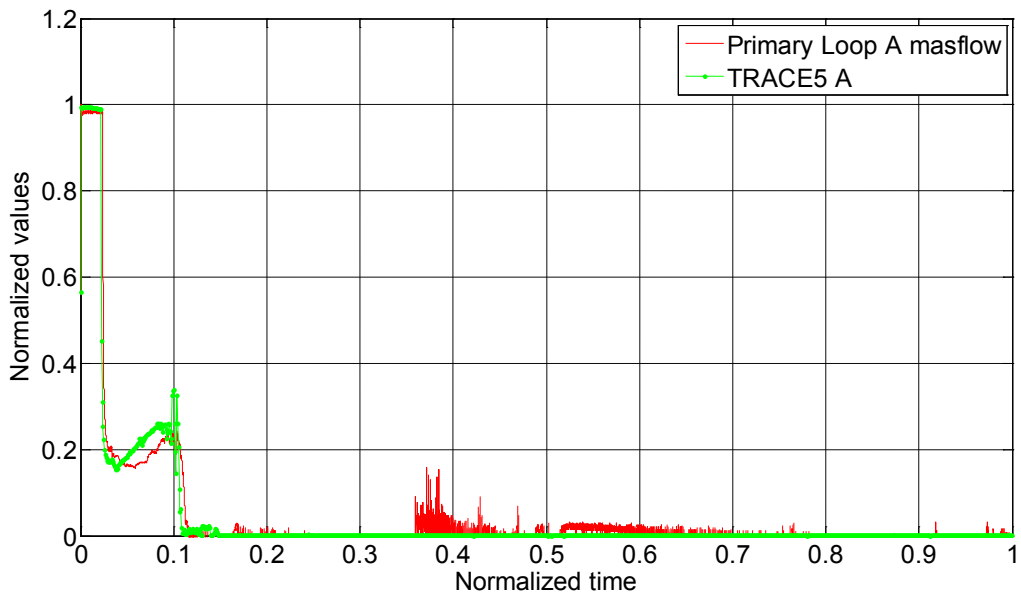


**Figure 8 Primary mass flow, loop A (0.0 to 1.0 NT)**

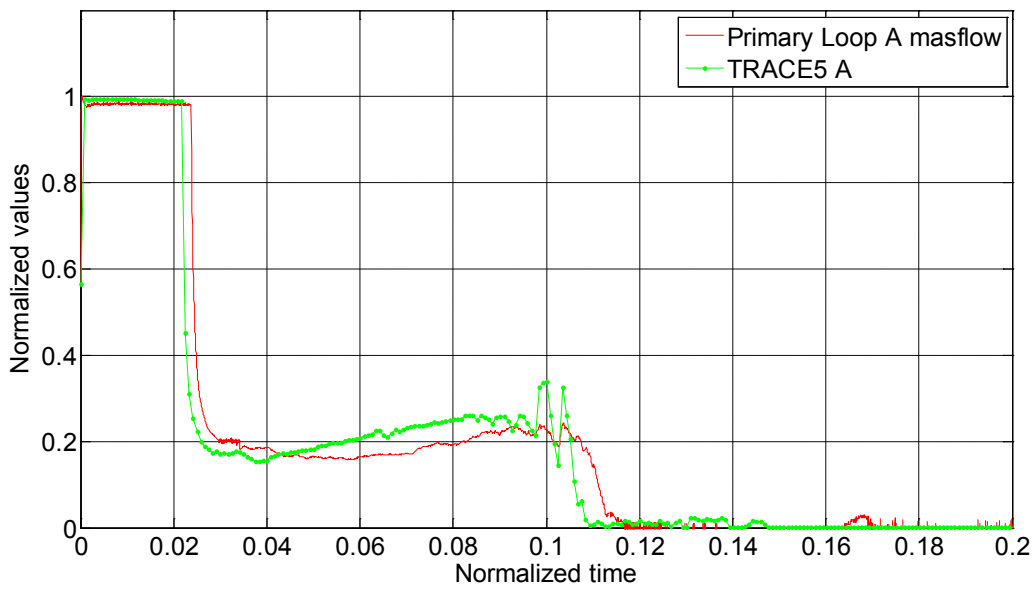


**Figure 9 Primary mass flow, loop A (0.0 to 0.2 NT)**

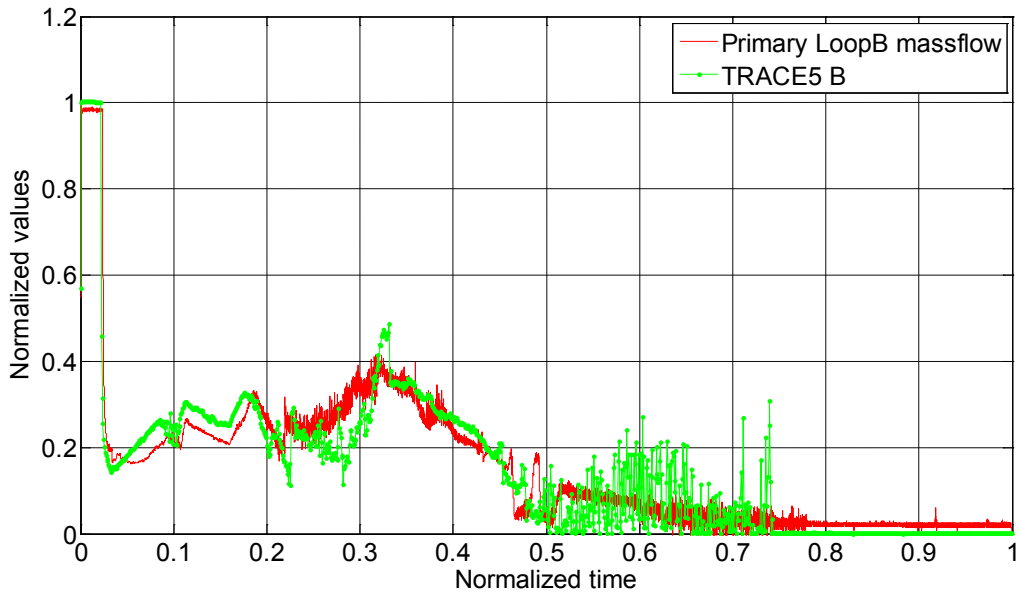


**Figure 10 Primary mass flow, loop B (0.0 to 1.0 NT)**

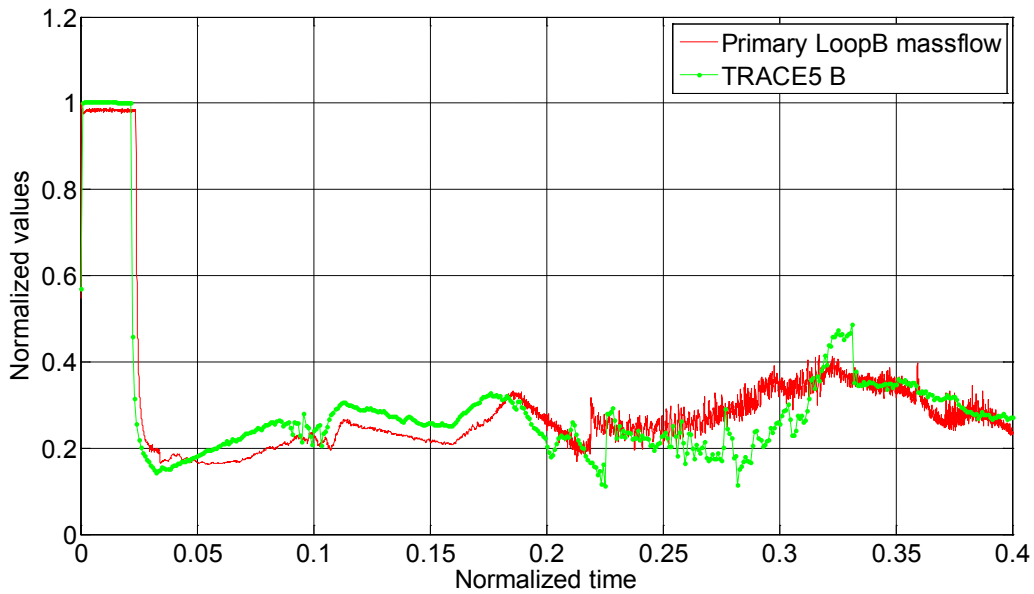


**Figure 11 Primary mass flow, loop B (0.0 to 0.4 NT)**

In the previous figure two consecutive flow stagnations (in loop B at 0.44 NT and 0.47 NT in the experiment) are shown, during the gas inflow process. Due to the inadequate reproduction of nitrogen transport with TRACE, loop B flow stagnation during the gas inflow is not properly reproduced.

## 5.6 Vessel collapsed liquid levels

The following figures show a comparison between the collapsed liquid levels in the upper plenum, core and downcomer, respectively for both experimental and TRACE results. In the experiment, the collapsed liquid level is computed from differences in pressure between the upper and lower parts of each region, and the coolant densities. The collapsed water level decreased due to a loss of the AIS coolant inventory through the break.

It is clearly shown that TRACE adequately reproduces all collapsed liquid levels during the first and second part of the transient (until gas inflow in the primary circuits). However, when nitrogen inflow starts, TRACE predicts a collapsed liquid drop in the upper plenum, which is not registered in the experiment.

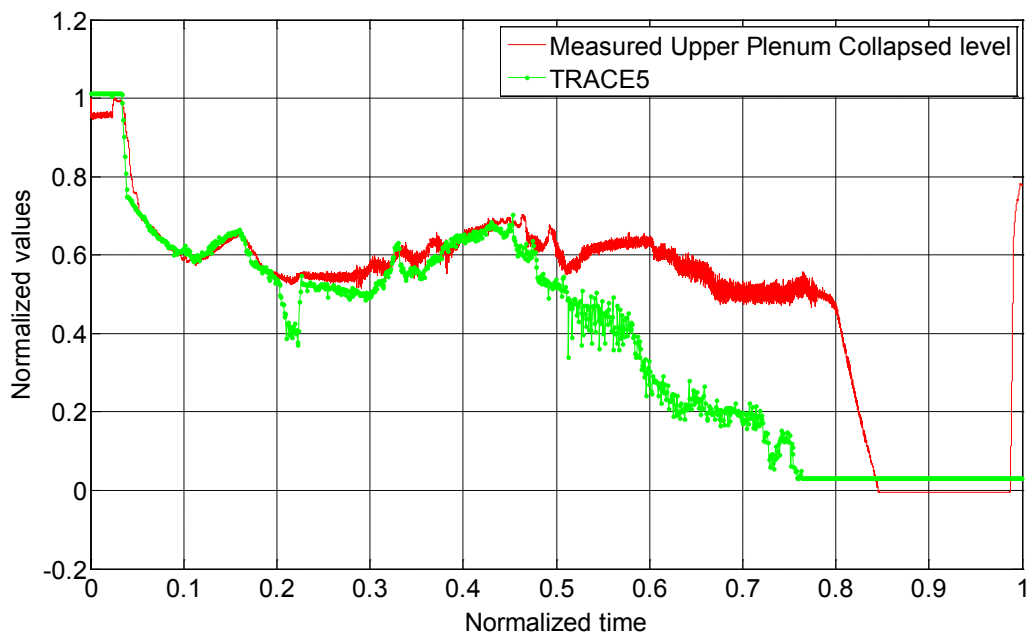


**Figure 12 Upper plenum collapsed liquid level (0.0 to 1.0 NT)**



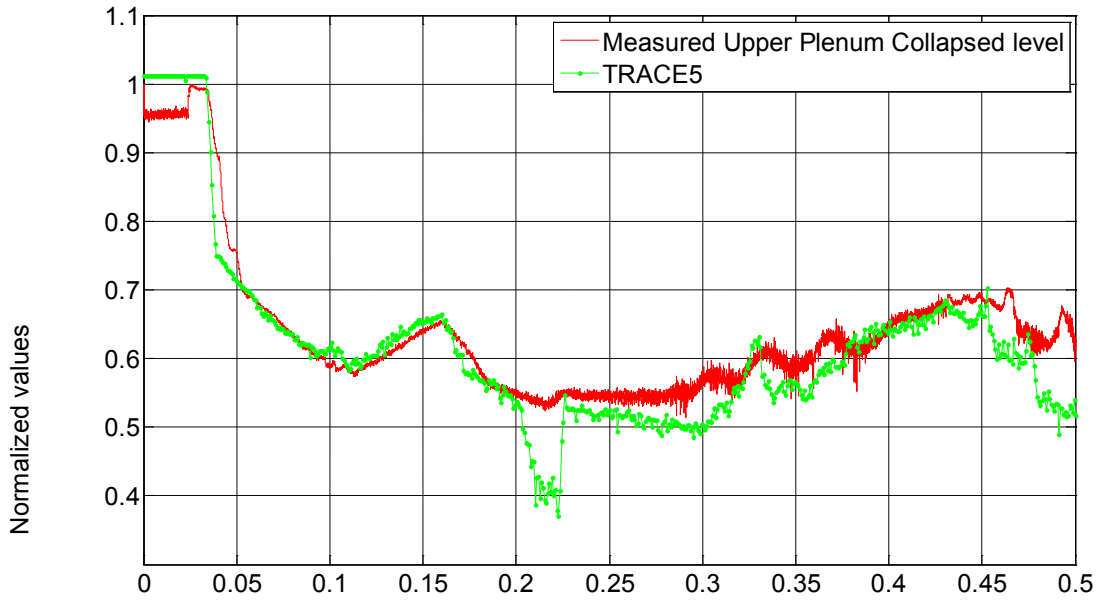


**Figure 13 Upper plenum collapsed liquid level (0.0 to 0.5 NT)**

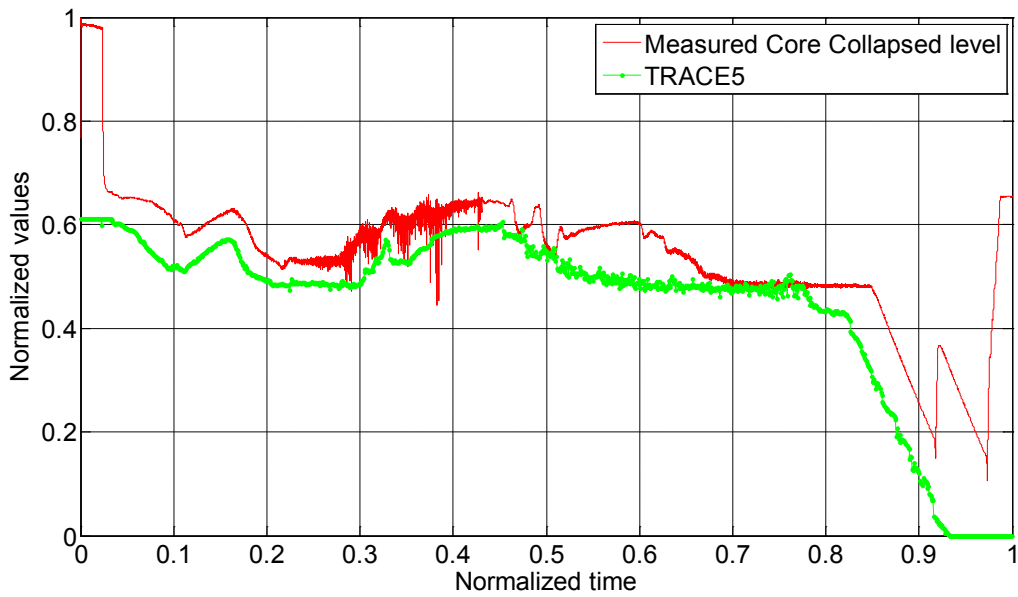


**Figure 14 Core collapsed liquid level (0.0 to 1.0 NT)**

Simultaneously with the TRACE upper plenum drop, also downcomer starts to decrease its liquid level, underpredicting one meter during the rest of the transient.

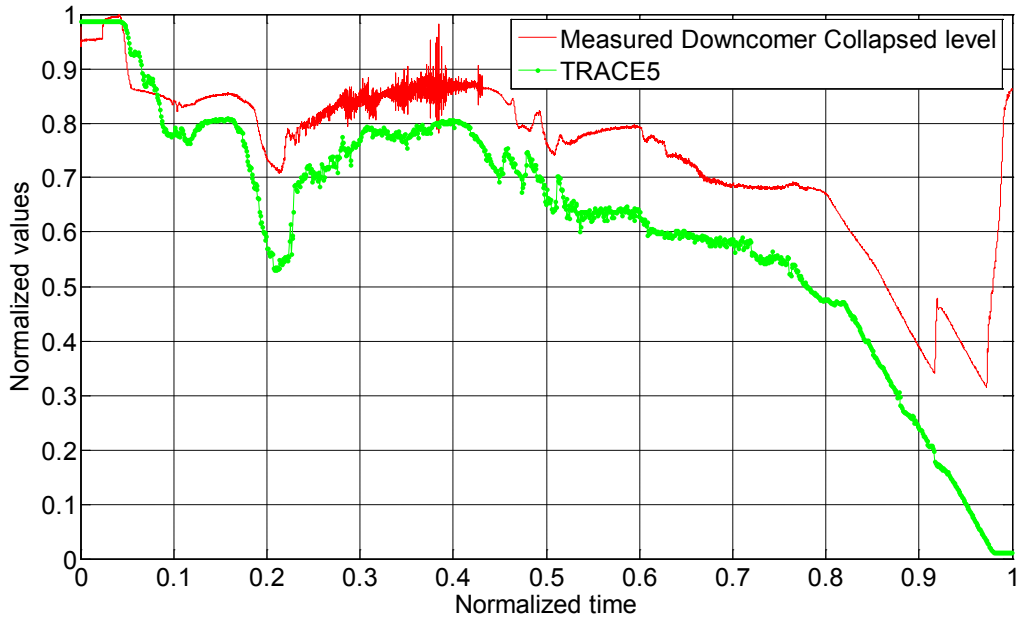


**Figure 15 Downcomer collapsed liquid level (0.0 to 1.0 NT)**

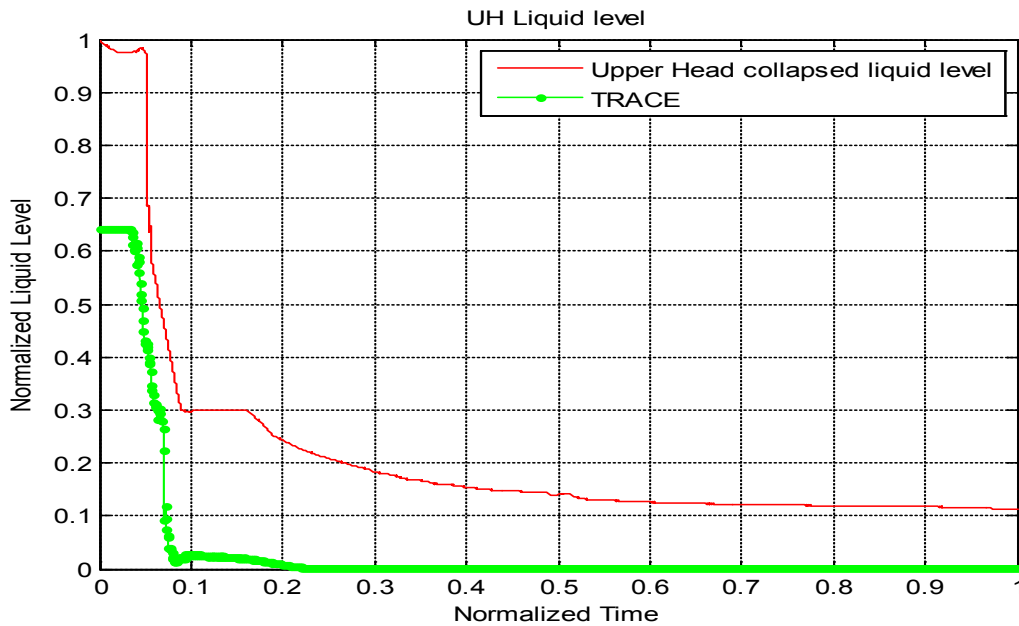


**Figure 16 Upper head collapsed liquid level**

Upper head liquid level is shown in figure 16. Experimentally, collapsed liquid level in upper head is obtained by difference of pressures between the condensing pot level (9.653 m) and the upper support plate (6.170 m). This value is compared with the one obtained by TRACE, between the upper head top (8.600 m) and the core support plate (6.170 m). The different upper levels used for measurements in the experiment, justifies the apparent disagreement between both curves. In the

experiment, liquid level decreases sharply at the beginning of the transient and stops at the level of spray nozzle top, indicating steam discharge from the upper head to downcomer. This effect is not well reproduced by TRACE5.

## 5.7 Peak cladding temperature

TRACE correctly reproduces the evolution of the maximum fuel rod temperature in the core. The maximum temperature is reached at 0.88 NT. At this moment, the core protection system activation is produced, reducing the core power according to a programmed decay power curve (figure 18 and table 5). TRACE fuel rod surface temperature is in good agreement with experimental values (figure 17).

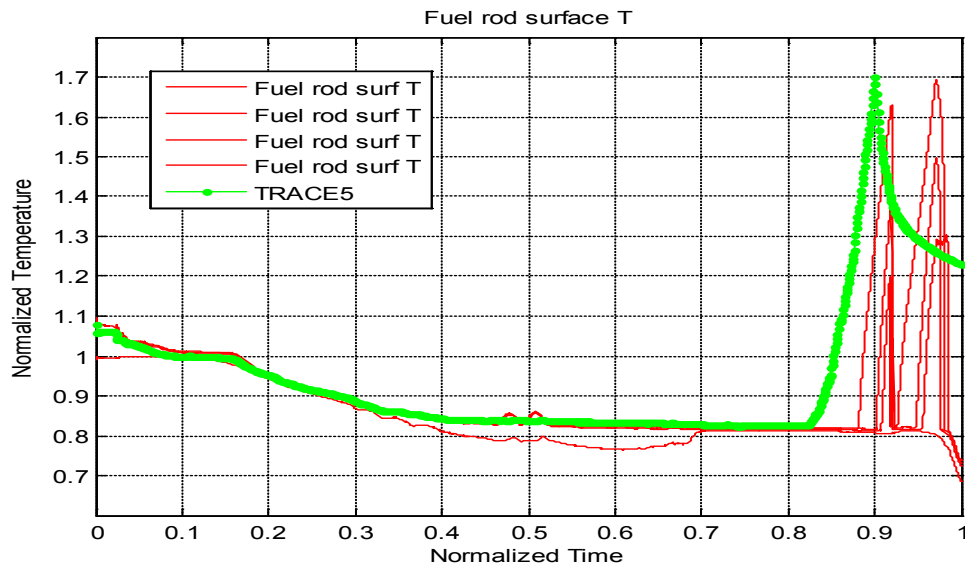


**Figure 17 Maximum fuel rod surface temperature**

However, at the end of the experimental transient during the LPI actuation, a repeated core quench process is produced, which is not reproduced by TRACE due to the fact that the pressure conditions to the activation of LPIs is not reached in the simulation.

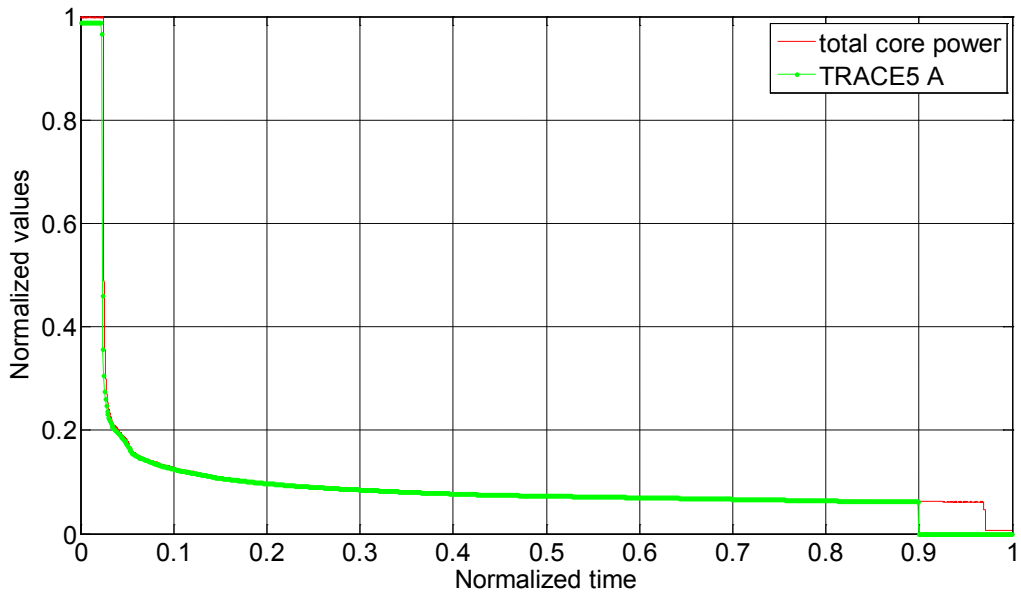


**Figure 18 Core power (0.0 to 1.0 NT)**

### **5.8 Hot and cold legs liquid levels**

The following figures show the liquid level in hot and cold legs, respectively. Experimentally, liquid level was obtained with a three gamma ray beam densitometer.

It is shown that hot leg liquid levels are similar in the two loops, irrespective of the different loop flow conditions (flow stagnation in loop A and natural circulation flow in loop B). TRACE5 reproduces this effect successfully. At 0.2 NT collapsed liquid level starts to increase due to accumulator's water injection. Fluctuations in liquid level due to nitrogen entrance are registered mainly in loop A.

Collapsed liquid level has been calculated measuring the void fraction in different cells. For this calculation curvature of pipe was not taken into account.

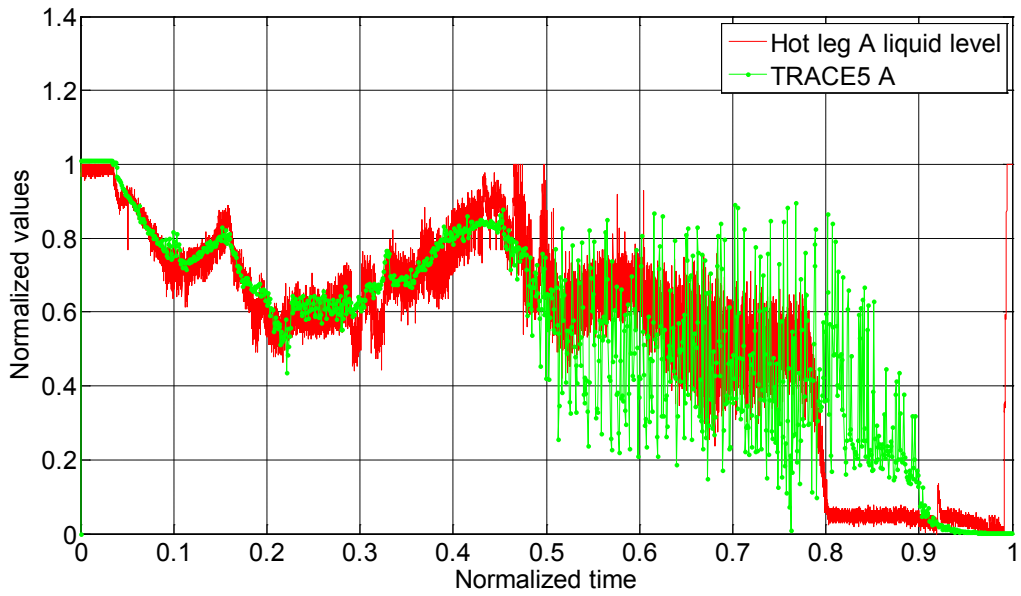


**Figure 19 Collapsed liquid level in hot leg A (0.0 to 1.0 NT)**

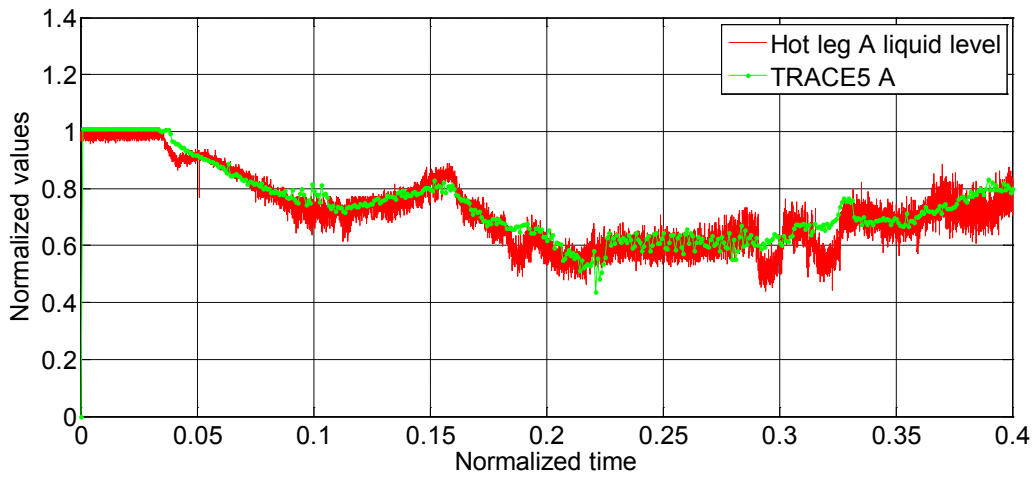


**Figure 20 Collapsed liquid level in hot leg A (0.0 to 0.4 NT)**

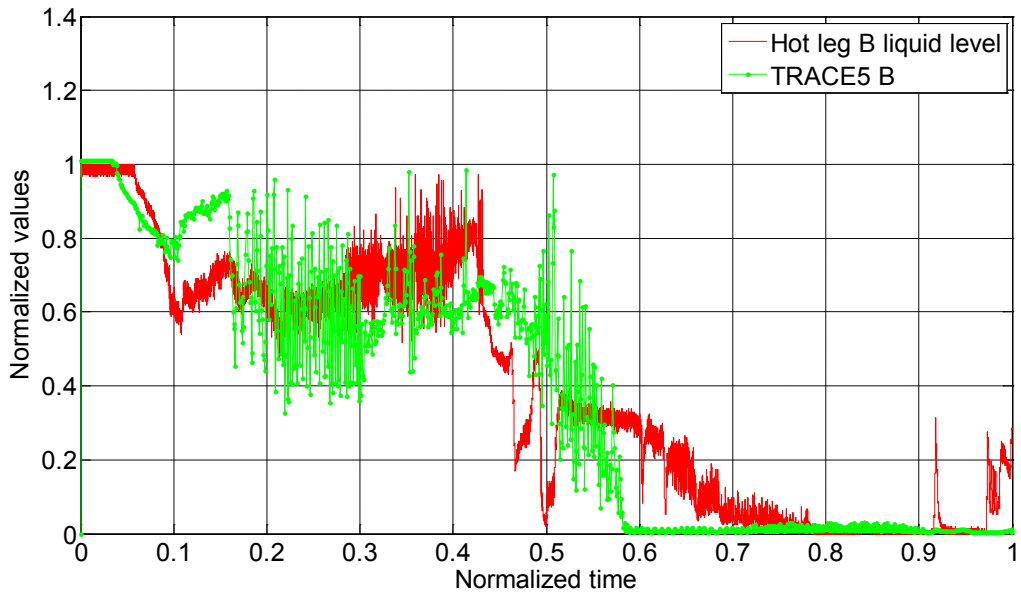


**Figure 21 Collapsed liquid level in hot leg B (0.0 to 1.0 NT)**

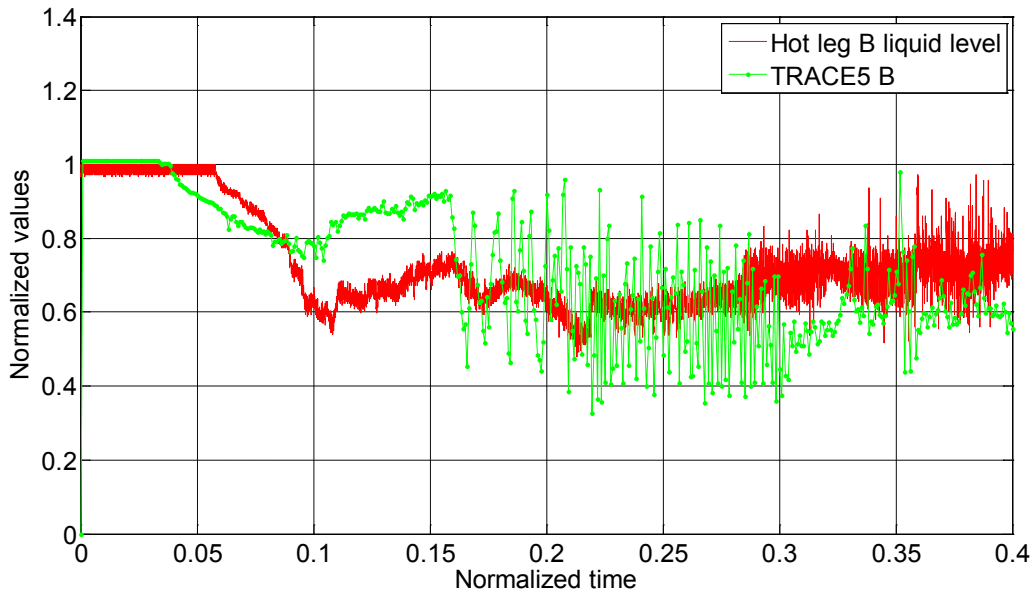


**Figure 22 Collapsed liquid level in hot leg B (0.0 to 0.4 NT)**

In the cold leg liquid level graphics, an increase of level between 0.2 NT and 0.4 NT due to the entrance of water from accumulators can be observed. In this case, differences between loop A and B are more important, especially at 0.4 NT, when the accumulators become empty.

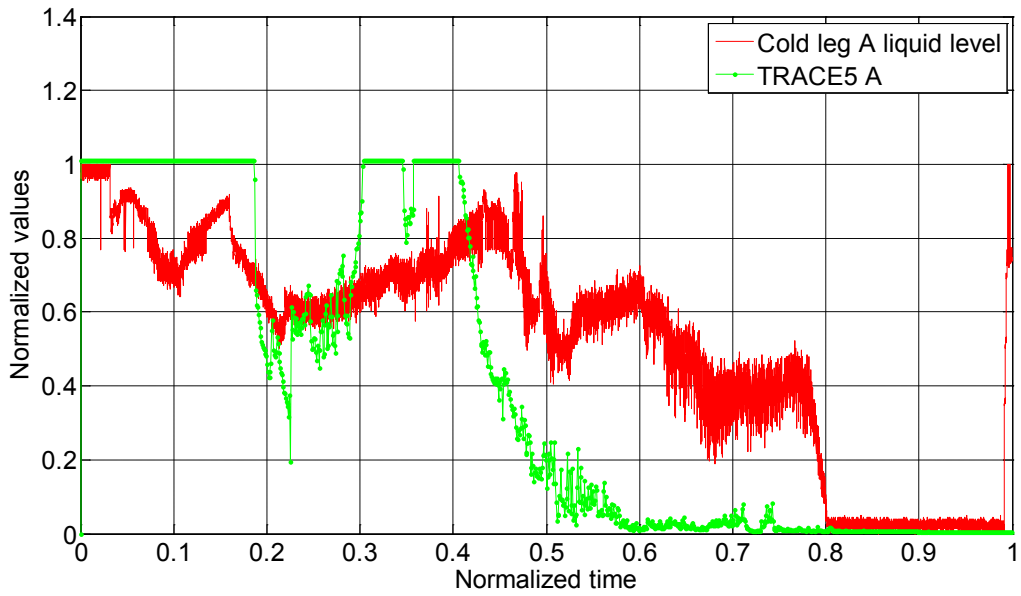


**Figure 23 Collapsed liquid level in cold leg A (0.0 to 1.0 NT)**

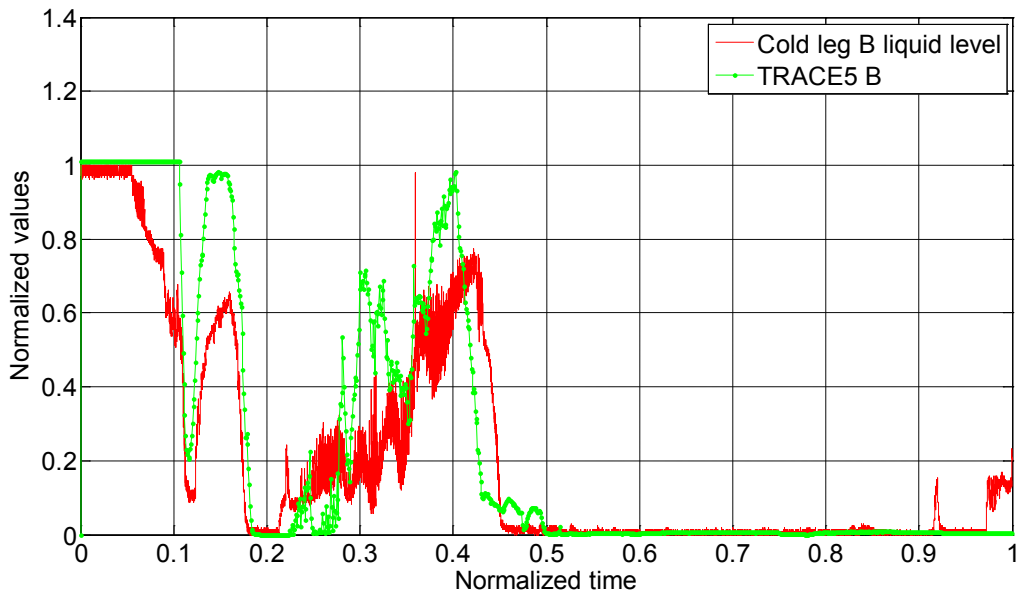


**Figure 24 Collapsed liquid level in the cold leg B (0.0 to 1.0 NT)**

## 5.9 Steam Generator main steam mass flow rate

The main steam isolation valves are fully closed when the scram signal is generated. A good reproduction of the mass flow through the MSIVs of both steam generators has been achieved, as it can be seen in figures 25, 26, 27 and 28.

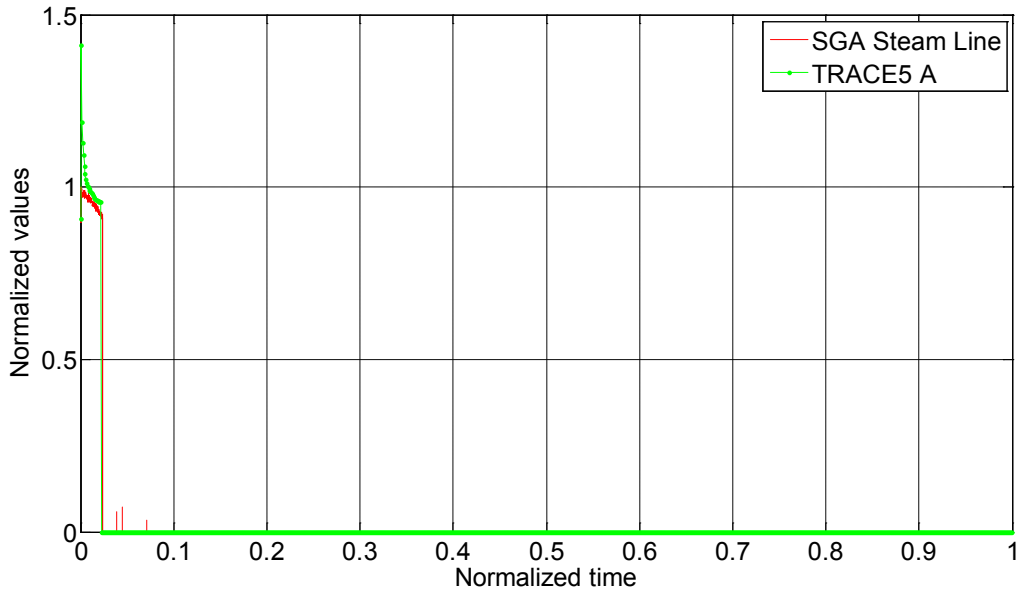


**Figure 25 Steam mass flow through the main line (0.0 to 1.0 NT)**

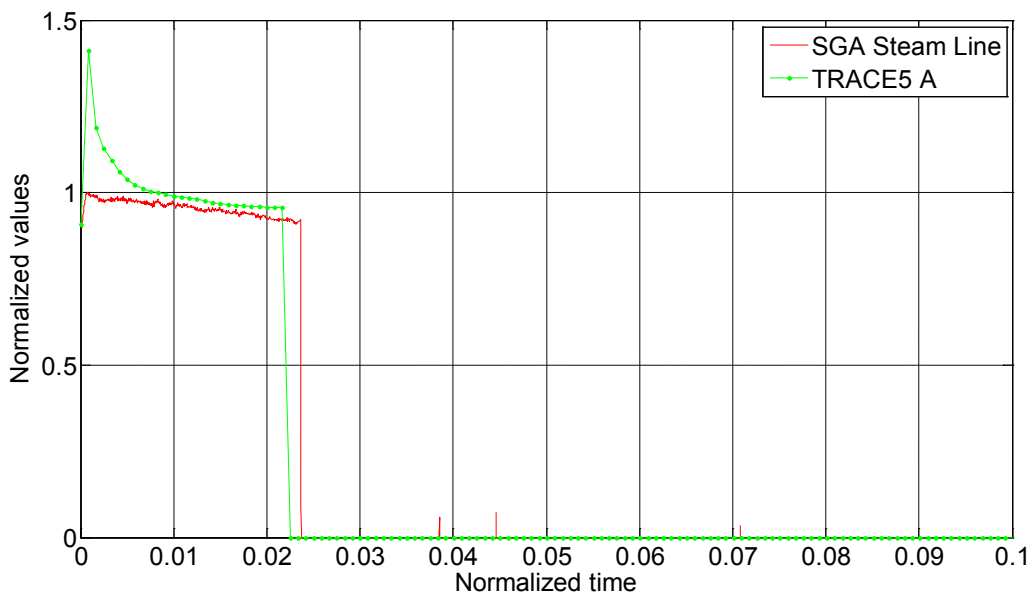


**Figure 26 Steam mass flow through the main line (0.0 to 0.1 NT)**



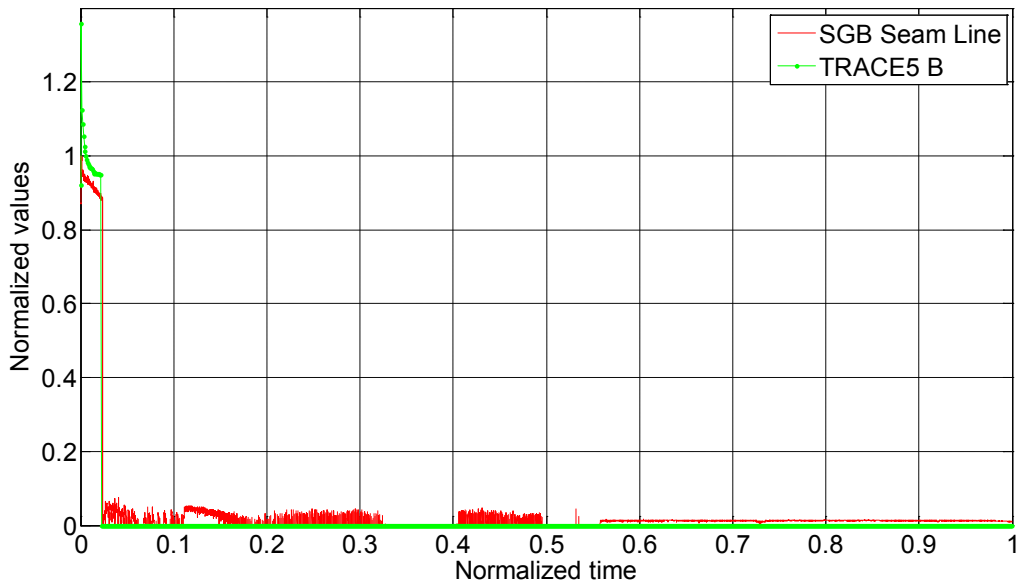


**Figure 27 Steam mass flow through the main line (0.0 to 1.0 NT)**

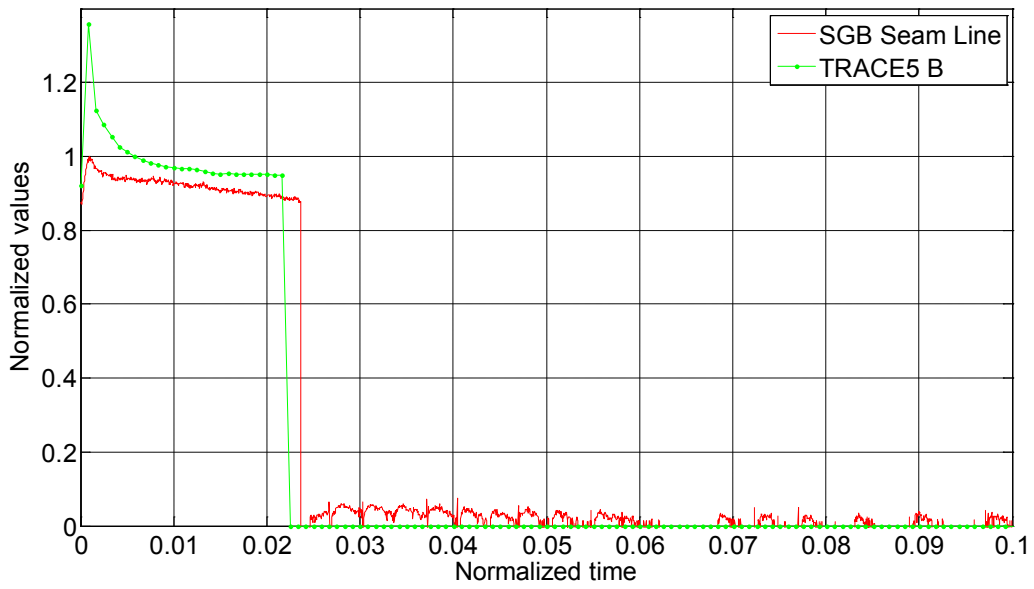


**Figure 28 Steam mass flow through the main line (0.0 to 0.1 NT)**

## 5.10 Steam Generator relief valve flow rate

A good agreement has been achieved between TRACE and the experiment, as it can be observed in figures 29, 30, 31 and 32. These figures perfectly show the periods corresponding to the relief valves actuation. An apparent disagreement between TRACE and experimental value can be seen in figure 31. This discrepancy is due to the location of the signal which measures the steam mass flow in the model. In the curve corresponding to TRACE, the mass flow through RV of SGB is represented and therefore flow through AM valve is not included.

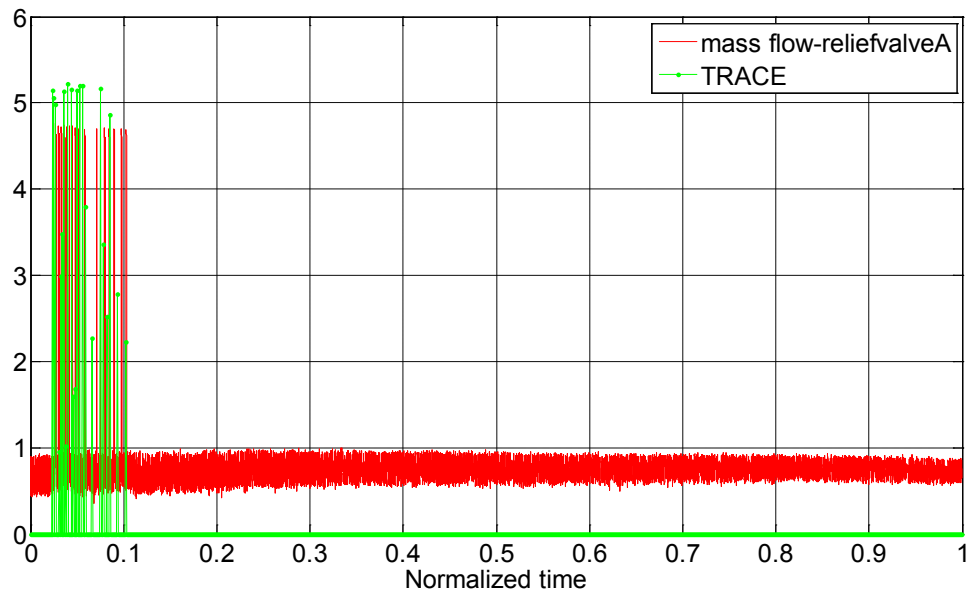


**Figure 29 SG A relief valve mass flow rate (0.0 to 1.0 NT)**

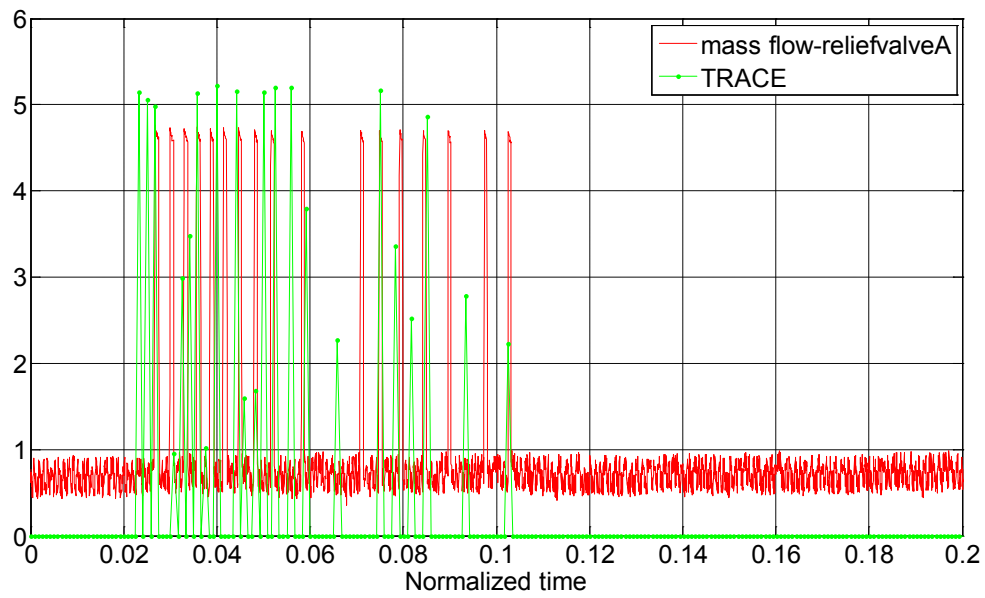


**Figure 30 SG A relief valve mass flow rate (0.0 to 0.2 NT)**

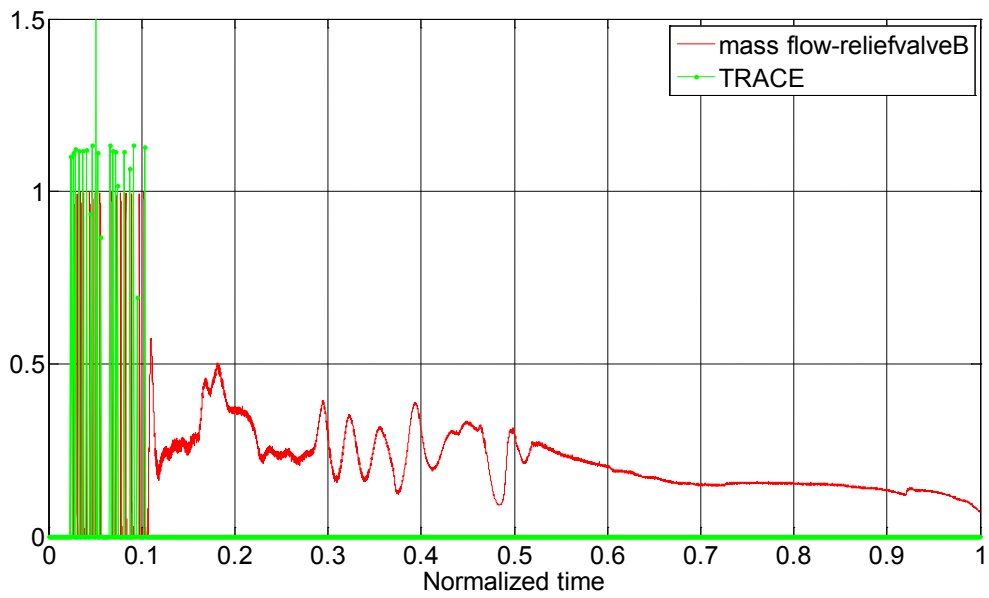


**Figure 31 SG B relief valve mass flow rate (0.0 to 1.0 NT)**

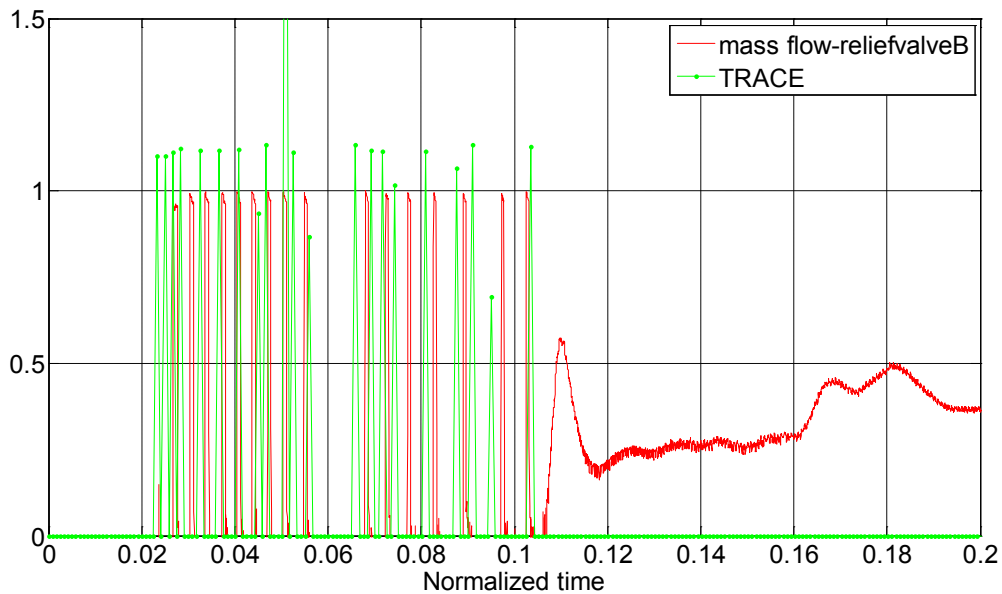


**Figure 32 SG B relief valve mass flow rate (0.0 to 0.2 NT)**

### **5.11 Steam generator U-tubes collapsed liquid level**

U-tubes have been grouped according to similar lengths. Experimentally 6 types were considered. In the TRACE simulation and due to the calculation time cost together with the obtained results, a 3-group classification has been adopted. Figures 33, 34, 35, 36, 37 and 38 show a comparison between the experimental and the simulated U-tube liquid level of SG A and SG B.

The collapsed liquid level in the U-tubes of SG A and B show a completely different behavior. Collapsed liquid level in U-tubes (SG A) started to decrease after the inlet plenum fluid temperature reached the saturation condition and became completely empty at 0.16 NT, as can be seen in the following figures. In this moment the mass flow through the primary side of loop A almost disappears, only existing steam natural circulation. On the other hand, the behavior of the up-flow (inlet) and down-flow (outlet) sides is quite similar. The signal type used by TRACE, which allows measuring collapsed liquid level only in vertical cells, produces the difference in level during the first part of the transient. This is because the cells in the top of the U-tubes (not vertical) are not considered by the signal. After the top level is emptied, the values become almost the same for both TRACE5 simulation and the experiment.

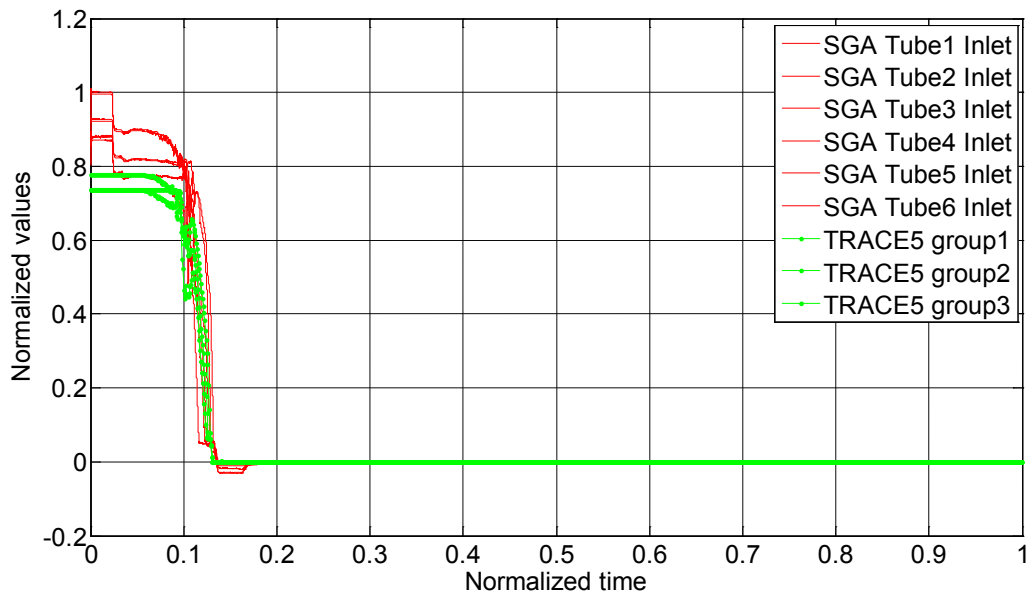


**Figure 33 Collapsed liquid level in the U-tubes of the SG A. Inlet (0.0 to 1.0 NT)**

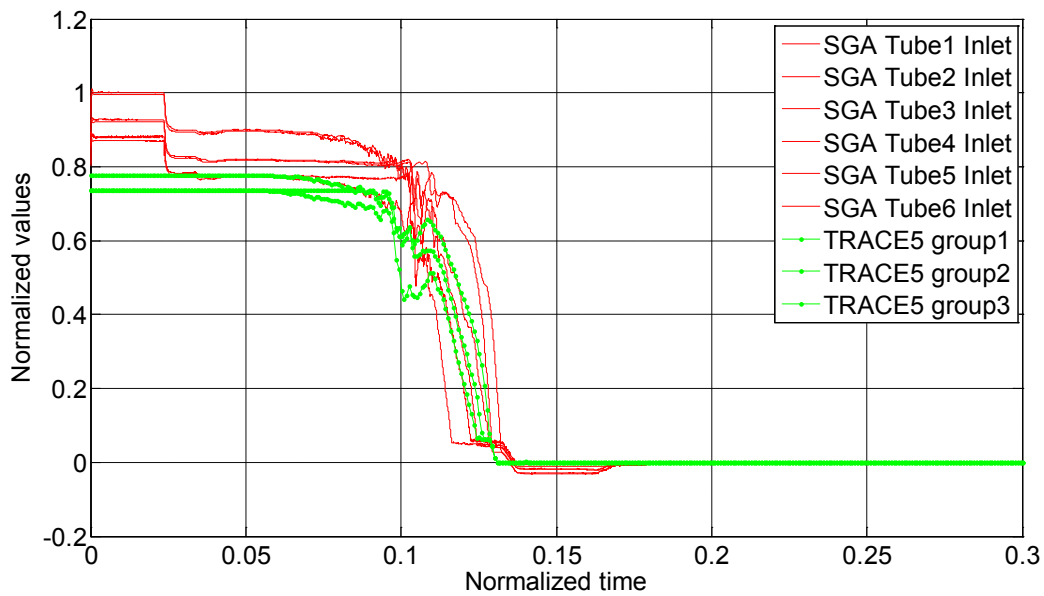


**Figure 34 Collapsed liquid level in the U-tubes of the SG A. Inlet (0.0 to 0.3 NT)**

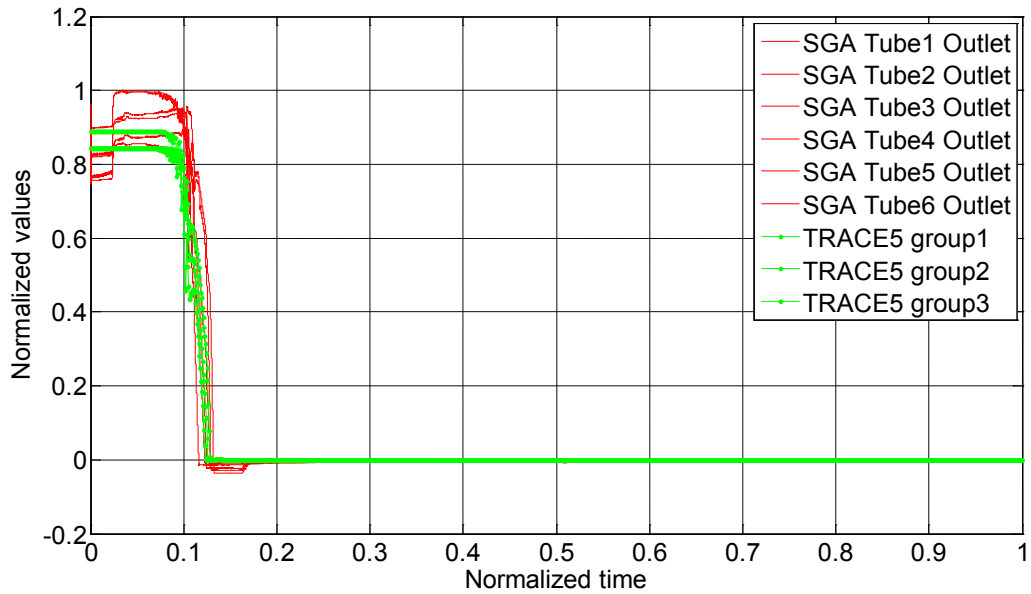


**Figure 35 Collapsed liquid level in the U-tubes of the SG A. Outlet (0.0 to 1.0 NT)**

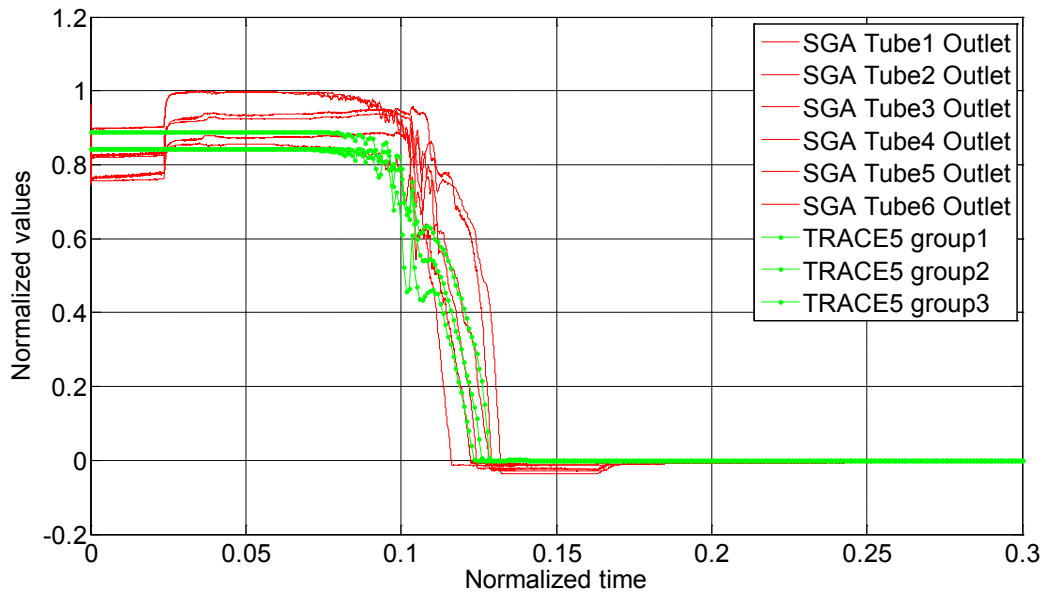


**Figure 36 Collapsed liquid level in the U-tubes of the SG A. Outlet (0.0 to 0.3 NT)**

Figures 37 and 38 show the collapsed liquid level in U-tubes of SG B. In both experimental and simulated cases, liquid level started to decrease at 0.16 NT indicating two-phase natural circulation conditions, recovering the top level during the auxiliary feedwater injection system actuation. Furthermore, the collapsed liquid level is slightly different depending on the longitude of the considered tube. TRACE also reproduces this situation successfully, as the following figures show.

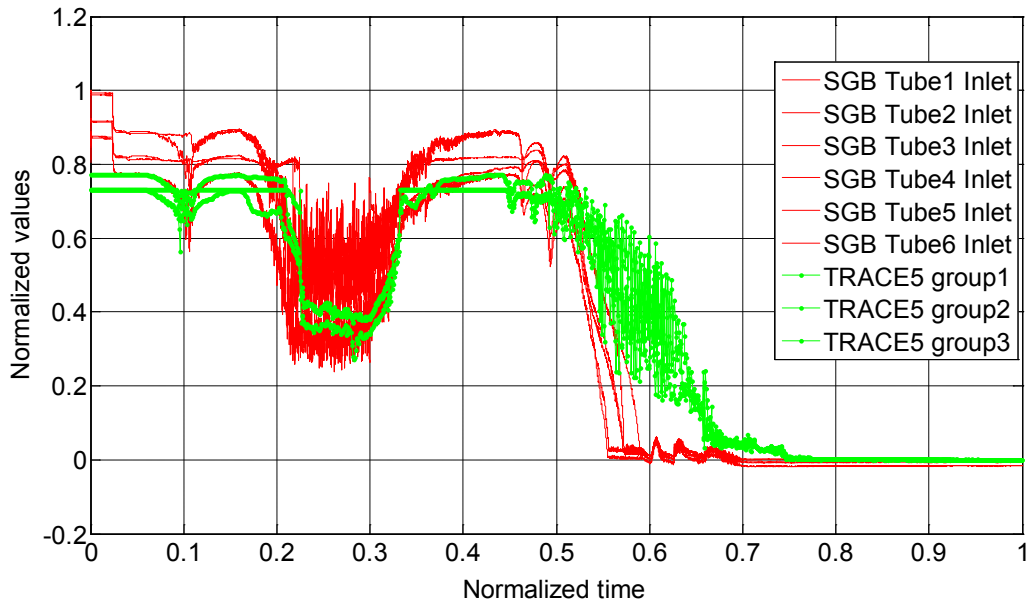


**Figure 37 Collapsed liquid level in the U-tubes of the SG B. Inlet (0.0 to 1.0 NT)**

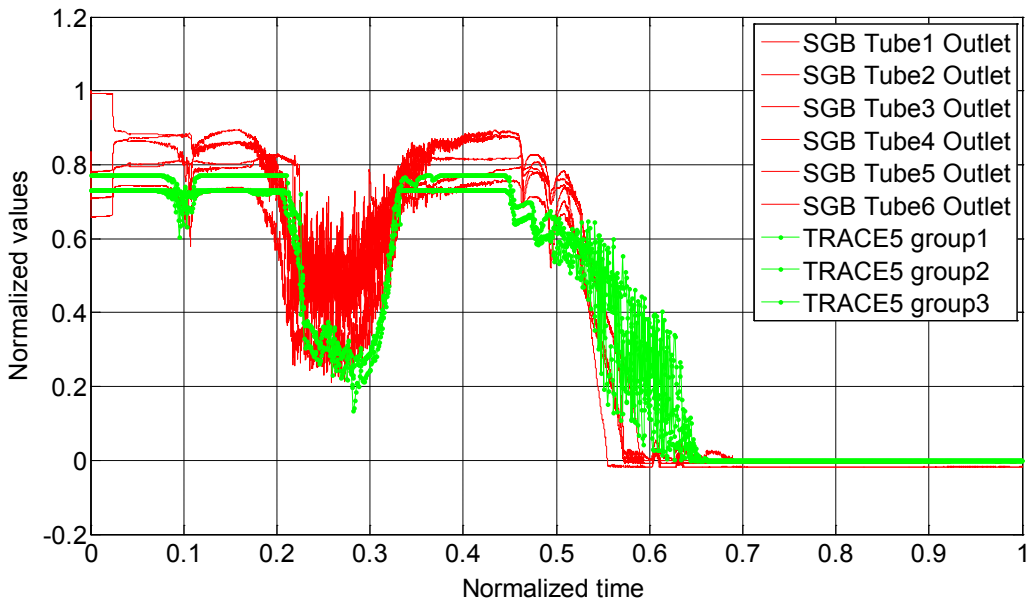


**Figure 38 Collapsed liquid level in the U-tubes of the SG B. Outlet (0.0 to 1.0 NT)**

It is important to remark that strong fluctuations are registered with TRACE, when gas nitrogen is introduced into the primary circuit.

## 5.12 Steam generators secondary-side liquid level

The following figures (39, 40, 41 and 42) show the collapsed liquid level of the secondary side of the steam generator. Experimentally, the liquid level is kept above the U-tubes. The behaviour of each steam generator is completely different. SG A liquid level slightly decreased after the RV closure at 0.108 NT. SG B secondary-side liquid level decreases after the start of the continuous steam discharge through the AM valve. In both cases, TRACE successfully reproduces the behaviour during the entire transient.

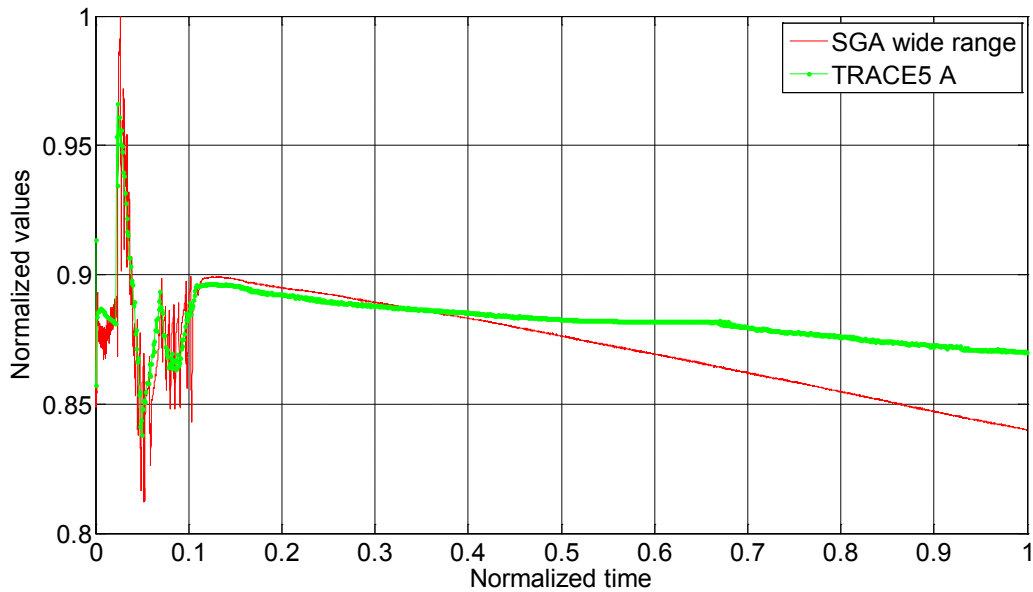


**Figure 39 Steam generator A. Secondary-side collapsed liquid level (0.0 to 1.0 NT)**



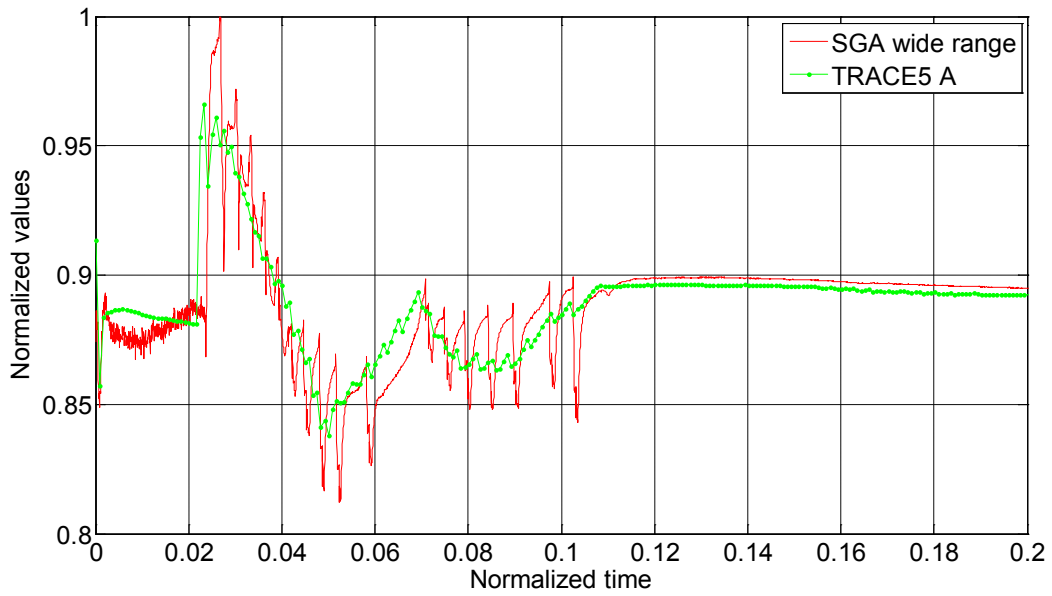


**Figure 40 Steam generator A. Secondary-side collapsed liquid level (0.0 to 0.2 NT)**

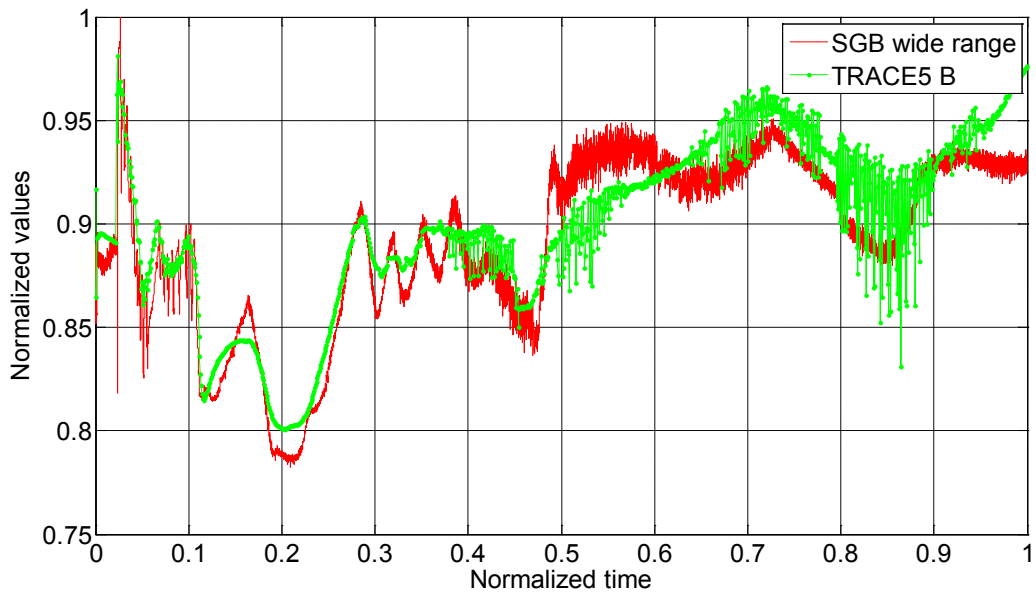


**Figure 41 Steam generator B. Secondary-side collapsed liquid level (0.0 to 1.0 NT)**

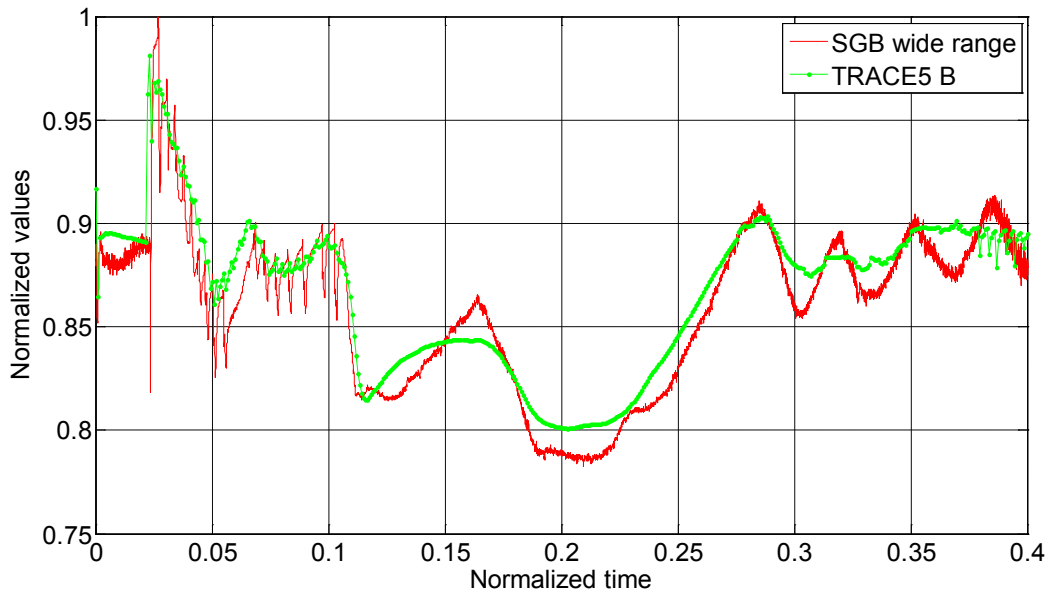


**Figure 42 Steam generator B. Secondary-side collapsed liquid level (0.0 to 0.4 NT)**

### 5.13 Pressurizer liquid level

Figure 43 shows the PZR water level. The liquid level of the PZR decreases immediately after the break, becoming fully empty at 0.028 NT. Furthermore, heaters of the PZR automatically connect to the maximum power after the break, following the logic control of the transient depressurization. Heaters are disconnected at 0.013 NT by the signal of minimum level of the PZR. The liquid level of the PZR shows a temporal recovering at 0.023 NT, concurrent with the increment of pressure of the primary, due to the primary coolant expansion when the temperature of the secondary rises, after the closure of the MSIVs.

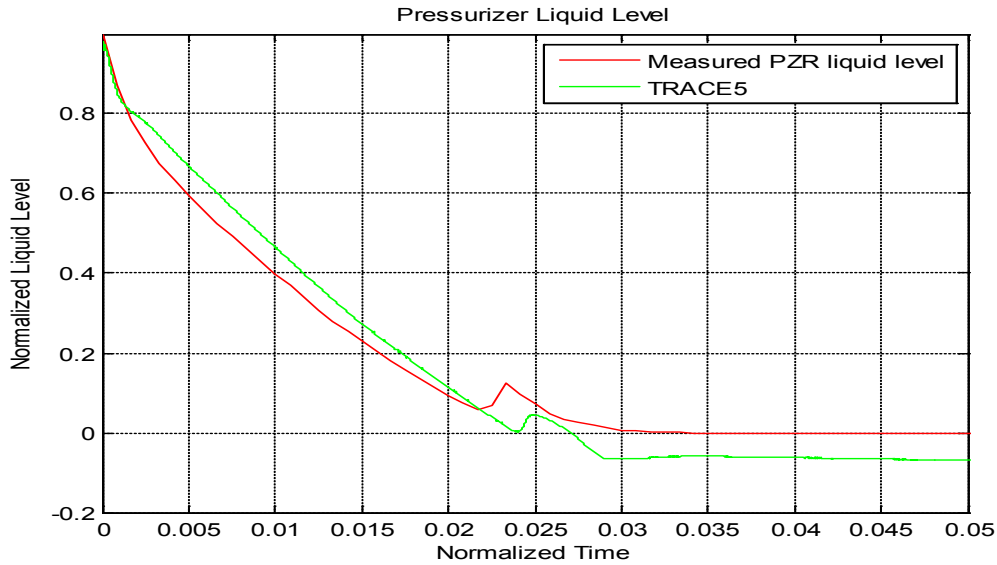


**Figure 43 PZR liquid level**

**5.14 Accumulator liquid level**

Figures 44 and 45 show the accumulators collapsed liquid level. The AIS starts the injection of coolant from the accumulator tanks at 0.204 NT, when the primary pressure falls below 0.28 NV. Injection finishes at 0.4 NT, starting the continuous nitrogen-gas flowing through accumulators into both cold legs. In any case, a good agreement between experimental and TRACE predicted values can be seen.

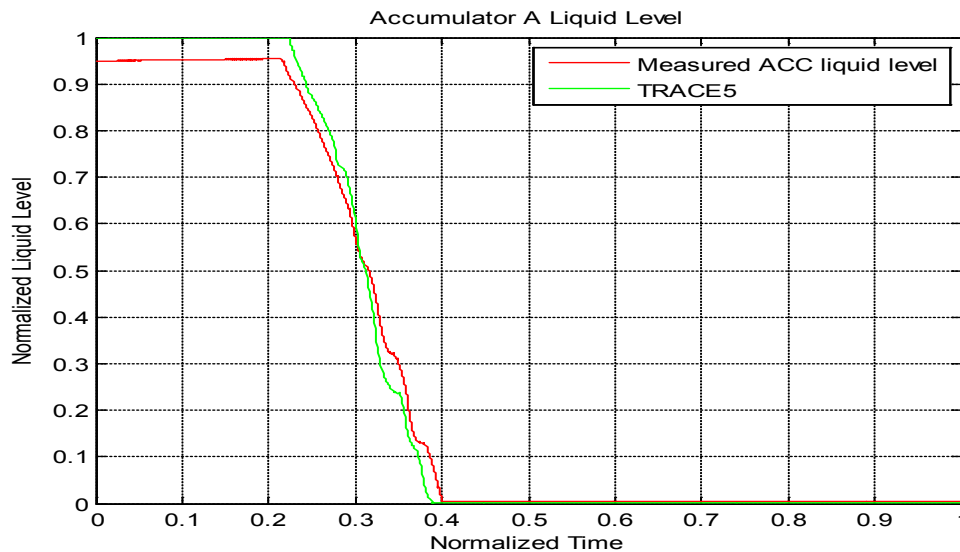


**Figure 44 Accumulator liquid level in loop A**

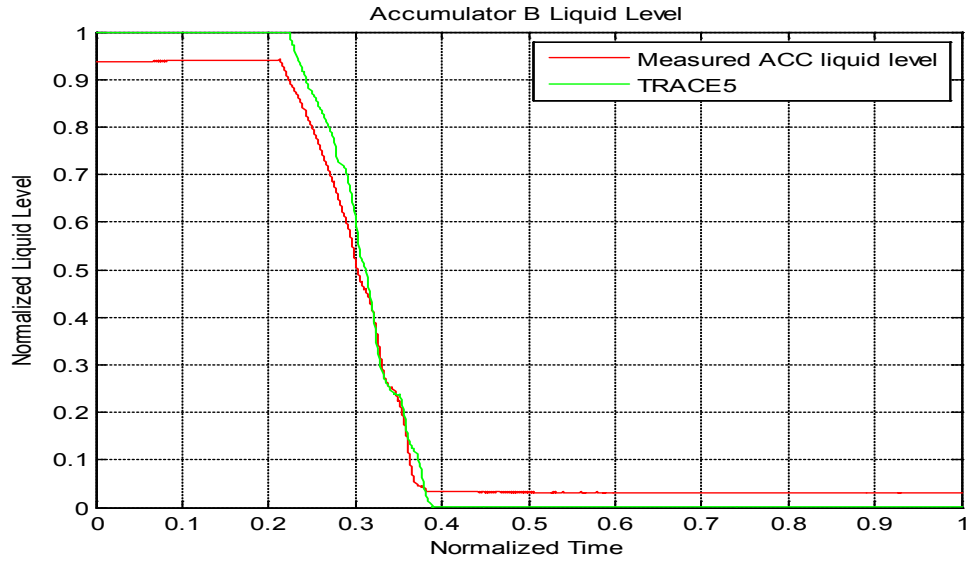


**Figure 45 Accumulator liquid level in loop B**

**5.15 Hot leg temperature**

Figure 46 shows the temperature of the fluid in the hot leg of loop A. The most remarkable discrepancy is registered during the period of injection of nitrogen, at which a slight overestimation with TRACE is observed.

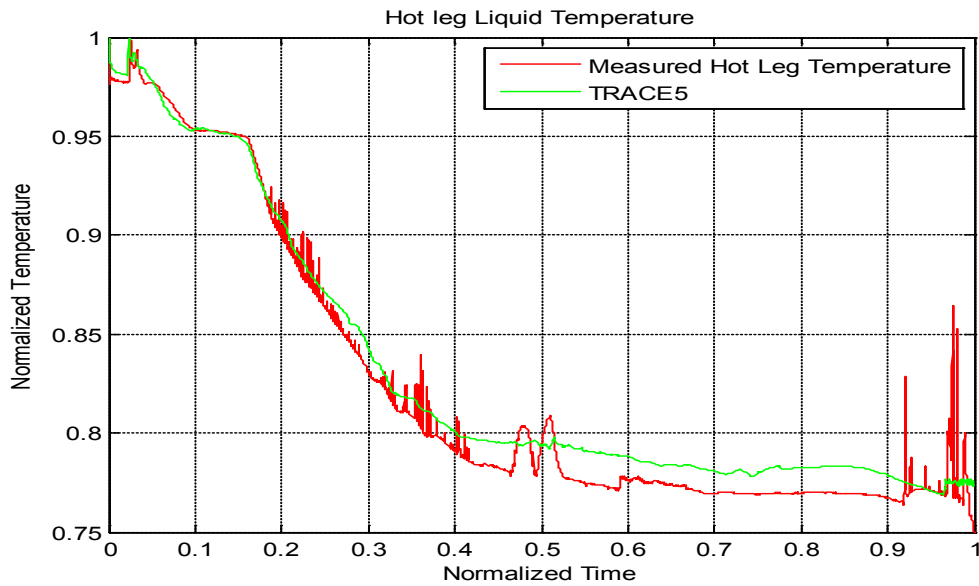


**Figure 46 Maximum hot leg fluid temperature**

In Figure 10 it is shown the primary mass flow rate in loop B. When accumulators are empty and N<sub>2</sub> injection starts (0.4-0.5 NT), it can be observed that the predicted mass flow rate is lower than the experimental one. Furthermore, collapsed liquid level in U-tubes of SG-B between 0.5 and 0.7 NT is higher than the experimental measurement (Figures 37 and 38). In summary, it seems that natural circulation is not properly simulated in this situation. Mass flow rate is underpredicted and consequently fluid temperature is increased (See Figure 46). This increase of temperature and pressure also contributes to not reach the LPI set point at the end of the transient.

## 5.16 Downcomer fluid temperature

Regarding the fluid temperature in the downcomer (Figure 47), the most remarkable discrepancy is observed at the level of 5.5 meters, in which the temperature of the fluid with TRACE is again slightly higher than the experimental during the injection of nitrogen. Similar tendencies are registered in the upper plenum and the lower plenum of the vessel. The accumulation of non-condensable gas in the U-tubes top, produces an increasing of pressure and therefore an increasing of the primary fluid temperature. This increase can be seen in the following figure at 0.44 NT and 0.48 NT in the experimental curve. This effect has not been reproduced with TRACE5.

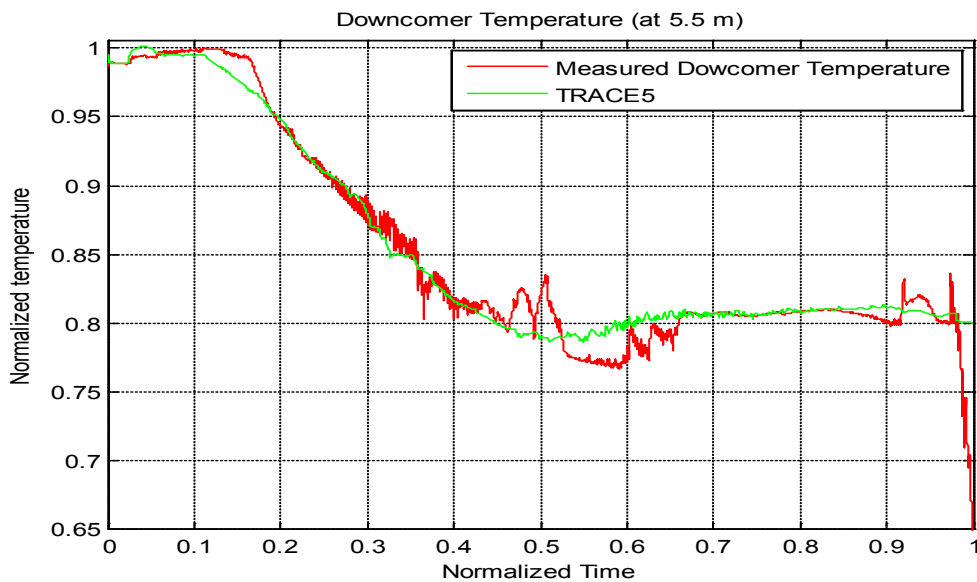


Figure 47 Downcomer fluid temperature (level 5.5 m)



## 6 CONCLUSIONS

This paper contains results obtained in the simulation of the OECD/NEA ROSA Project Test 6-2 with the code TRACE5. One of the goals of the work is to investigate the effectiveness of the secondary-side depressurization operation during a SBLOCA of a PWR, followed by an unlikely total failure of HPI, using experimental data from the integral test facility LSTF together with TRACE5 code analyses. The secondary-side depressurization in such an accident scenario would have an effect on the primary-side, depressurizing it until the pressure at which the accumulator actuates. Despite this fact, it does not prevent the core from being overheated at the end of the transient, maybe due to the non-condensable inflow. A break at the reactor vessel bottom does not allow gas discharge until the whole vessel becomes empty of coolant. Non-condensable gas remained in the primary loops may cause significant degradation of the effects of AM actions.

Results show that TRACE5 can successfully reproduce complicated conditions of natural circulation and fluid stagnation in different loops, when a break flow in the lower pressurized vessel is produced. TRACE5 adequately predicts the mass flow and the coolant inventory discharged through the break. In this particular case, no change to steam single-phase is produced.

The main discrepancies have been found during the simulation of non-condensable gas transport, affecting to the pressurized vessel liquid levels (mainly to upper plenum and downcomer).





## 7 REFERENCES

1. Thermohydraulic Safety Research Group, Nuclear Safety Research Center, Japan Atomic Energy Agency, 2007. Final Data Report of ROSA/LSTF Test6-2 (0.1% Pressure Vessel Bottom Small Break LOCA Experiment SB-PV-10 in JAEA).  
  
[2] Suzuki, M., Takeda T., Asaka H., Nakamura H., Effects of Secondary Depressurization on Core Cooling in PWR Vessel Bottom Small Small Break LOCA Experiments with HPI Failure and Gas Inflow, *Journal of Nuclear Science and Technology*, Vol 43, 1, p 55-64, 2006.  
  
[3] The ROSA-V Group, 2003. JAEA-Tech. ROSA-V Large Scale Test Facility (LSTF) system description for the third and fourth simulated fuel. assemblies.  
  
[4] Nuclear Regulatory Commission, 2007a. TRACE V5.0. User's manual. Volume 1: Input Specification. Division of Risk Assessment and Special Projects. Office of Nuclear Regulatory Research. U. S.  
  
[5] Nuclear Regulatory Commission, 2007b. TRACE V5.0. Theory manual. Field Equations, Solution Methods and Physical Models. Division of Risk Assessment and Special Projects. Office of Nuclear Regulatory Research. U. S.  
  
[6] RELAP5/MOD3.3 code manual. Volume II: User's guide and input requirements. December 2001. U.S. Nuclear Regulatory Commission.  
  
[7] Wolfert, K., Teschendorff, V., Lerchl, G., et. al., 1989. The thermal-Hydraulic Code ATHLET for Analysis of PWR and BWR Systems, NURETH-4. Karlsruhe 1989. Proc. vol. II, 1234-1239, 1989  
  
[8] Micaelli, J.C., Barré, F., Bestion, D., CATHARE Code Development and Assessment Methodologies. *Trans. of the ANS, Winter Meeting San Francisco*, October 29-November 2, vol. 73, 509-510, 1995.  
  
[9] Stephen M. Bajorek, Nikolay Petrov, Katsuhiko Ohkawa, Arthur P. Ginsberg. "Realistic Small And Intermediate-Break Loss of Coolant Accident Analysis Using WCOBRA/TRAC". *Nuclear Technology* Vol. 136. Oct. 2001.  
  
[10] Chien-Hsiung Lee, I-Ming Huang, Chin-Jang Chang. "Using An IIST 1% Cold-Leg SBLOCA Experiment With Passive Safety Injection To Assess The RELAP5/MOD3.2 Code". *Nuclear Technology* Vol. 135. Aug. 2001.  
  
[11] Kyoo Hwan Bae, Guy Hyung Lee, Hee Cheol Kim, Quun S. Zee. "SBLOCA Long Term Cooling Procedure for the Integral Type PWR". *Annals of Nuclear Energy* 34 (2007) 333-338. March 2007.  
  
[12] Afshin Heyadat, Hadi Davilu, Jalil Jafari. "Loss of Coolant Accident Analyses on Tehran

Research Reactor by RELAP5/MOD3.2 code". Progress in Nuclear Energy 49 (2007) 511e528. 2007.

[13] Y. Koizumi, H. Asaka, H. Kumamaru, M. Osakabe, K. Tasaka, Y. Mimura, "Investigation of Break Orientation Effect During Cold Leg Small Break LOCA at ROSA-IV LSTF," J. Nucl. Sci. Technol. 25 1988.

[14] Mitsuhiro Suzuki, Takesi Takeda, Hideaki Asaka, Hideo Nakamura. "Effects of Secondary Depressurization on Core Cooling in PWR Vessel Bottom Small Break LOCA Experiments with HPI Failure and Gas Inflow". Journal of NUCLEAR SCIENCE and TECHNOLOGY, Vol. 43, No. 1, p. 55–64. 2006.

[15] Hiroshige Kumamaru, Yutaka Kukita, Hideaki Asaka. "RELAP5/MOD3 Code Analyses of LSTF Experiments on Intentional Primary-Side Depressurization Following SBLOCAS with Totally Failed HPI. NUCLEAR TECHNOLOGY VOL. 126. June 1999.